Dynamic Decode-and-Forward Relaying using Raptor Codes

Azad Ravanshid, Lutz Lampe*, and Johannes Huber

Lehrstuhl für Informationsübertragung, Universität Erlangen–Nürnberg, Germany

*Department of Electrical and Computer Engineering, University of British Columbia, Canada.

Email: {azad@LNT.de, Lampe@ece.ubc.ca, huber@LNT.de}

Abstract

Dynamic decode-and-forward (DDF) is a version of decode-and-forward relaying in which the duration of the listening phase at relays is not fixed. In this paper, we investigate half-duplex DDF relaying based on rateless codes. The use of rateless codes allows relays to autonomously switch from listening to the source node to transmitting to the destination node. We first revisit different signal combining strategies applied at the destination node, namely energy and information combining known from literature, and propose a new combining method which we refer to as mixed combining. The different combining methods give rise to different achievable rates, i.e., constrained channel capacities, for which we provide analytical expressions. The capacity analysis reveals the conditions under which mixed combining is superior and how it can be optimized. We then consider Raptor codes as a specific implementation of rateless codes and develop a density-evolution approximation to predict the data-rate performance of these codes in DDF relaying. Furthermore, we devise an optimization of the output symbol degree distribution of Raptor codes that is mainly used to benchmark the performance of Raptor codes with a fixed degree distribution. Numerical results for exemplary three-node and four-node relay networks show that the proposed mixed combining provides significant gains in achievable data rate and that Raptor codes with a fixed degree distribution are able to realize these gains and to approach closely the constrained-capacity limits.

Index Terms

Cooperative communications, dynamic decode-and-forward, relaying, rateless codes, Raptor codes, density evolution.

Part of this work was presented at the IEEE International Symposium on Information Theory (ISIT), Seoul, Korea, 2009.

I. Introduction

In the wake of advances in multiple-antenna transmission and with the ongoing evolution towards network communication theory, the study of cooperative communications in wireless networks has experienced a recent revival, e.g. [1]–[5]. Cooperative communications can achieve spatial diversity and multiplexing without requiring multiple-antennas to be collocated in a single device. The three-terminal relay channel, as the fundamental unit of cooperative communications, was introduced in the pioneering work [6] and thoroughly analyzed in [7]. Although early information theoretic studies on cooperative communications focussed on full-duplex relaying, in recent years a lot of research has been directed towards practical protocols based on half-duplex relaying, where the relay is not able to receive and transmit simultaneously, e.g. [1]–[4], [8]. Among the various strategies that enable relays to assist the source-to-destination communication link, the decode-and-forward (DF) strategy has attracted great attention. In DF, the transmission interval is divided into a listening phase, during which a relay only receives, and a collaboration phase, during which the relay transmits the successfully decoded source message. The duration of the listening phase can be predetermined [3], [4] or it can be adapted to the actual quality of the source-to-relay channel [8]–[11]. In case of the latter, and in the absence of channel state information (CSI) at the sender, the relay would decide on its own when to switch from listening to collaborating, which is also referred to as dynamic decode-and-forward (DDF) [10].

Recently, starting with [12], the application of rateless codes, in particular Luby transform (LT) and Raptor codes [13], [14], has been advocated to accomplish DDF with a flexible duration of the listening phase. While [12] considered the three-node relay channel with non-orthogonal source-to-destination and relay-to-destination channels, relaying with multiple relay nodes and orthogonal subchannels were studied in [15]. The assumption of orthogonal channels enables the use of two different signal combining schemes at receiving nodes (destination and relays) during the collaboration phase, which are referred to as energy combining (EC) and information combining (IC) in [15]. In the context of collaboration using fixed-rate codes, the concepts of EC and IC are also known as DF with repetition coding and coded cooperation, respectively [4].

In this paper, we study half-duplex DDF transmission using rateless codes. As in [15], we consider orthogonal source-to-destination and relay-to-destination channels, and as in [12], [15] we assume that the destination node knows when a relay starts to transmit, which can be accomplished by, e.g., assigning relay-specific spreading sequences. We first consider signal combining when multiple signals are received during the collaboration phase of DDF. We formulate EC and IC in a common framework and introduce a new combining scheme, which is a hybrid of EC and IC and which we refer to as mixed combining (MC). We derive the pertinent capacity limits

associated with the three combining schemes, for which, different from [15], we consider transmission with finite-size constellations. MC requires power allocation at individual relays (but not among multiple relays), for which we provide an optimal solution determined at the destination node and delivered to relays via a low-rate feedback. Such a feedback requirement is similar to the acknowledgment sent from the destination to terminate the transmission with rateless codes. Second, we analyze achievable rates for DDF using Raptor codes. To this end, we refine and extend the density evolution [16] method proposed in [17] to the case of DDF. In this context, we also investigate the optimization of the degree distribution of the LT component codes. This optimization is similar to that for fixed-rate low-density parity check (LDPC) codes considered in e.g. [18], [19], which are required to perform close to the capacity limit at different rates for the source-to-relay and source/relay-to-destination channel. We present numerical results for the examples of source-to-destination transmission assisted by one and two relays, respectively, which demonstrate (i) the notable advantage of the proposed MC over EC and IC, (ii) the aptitude of Raptor codes with fixed degree distributions to closely approach the capacity limits associated with DDF, and (iii) the suitability of the devised density evolution approximation to predict rates achievable with Raptor codes for DDF.

The remainder of this paper is organized as follows. In Section II we introduce the cooperative communications system setup and describe the combining schemes including our proposed MC method. In Section III, we derive the constrained capacity limits associated with DDF and different combining methods. A density evolution approximation for DDF transmission with Raptor codes is developed in Section IV, which also serves as the basis for the optimization of Raptor codes. Numerical results are presented and discussed in Section V, followed by conclusions in Section VI.

II. Relay Transmission and Signal Combining

In this section, we first briefly introduce the considered relay transmission system and then describe the signal combining schemes applied at the destination node.

A. System Setup

We consider a wireless relay network as shown in Figure 1 consisting of a source node S, N_{R} relay nodes R_i, $i = 1, \ldots, N_{\mathrm{R}}$, and a destination node D, to which the source wishes to communicate a message. For simplicity, we assume that all nodes employ a single antenna. The channels between different nodes are modeled as frequency-flat fading additive white Gaussian noise (AWGN) channels which remain constant during the transmission of at least one message. The instantaneous receiver-side signal-to-noise power ratio (SNR) for the

source-to-destination (SD), source-to-relay-i (SR_i), relay-i-to-relay-j ($\mathrm{R}_i\mathrm{R}_j$), and relay-i-to-destination ($\mathrm{R}_i\mathrm{D}$) channel is denoted by γ_{SD}, γ_{SR_i}, $\gamma_{\mathrm{R}_i\mathrm{R}_j}$, and $\gamma_{\mathrm{R}_i\mathrm{D}}$, respectively.

The operation of the relay network follows closely the one described in [15]. The relay nodes are half-duplex transceivers that apply the DDF paradigm to assist the source. That is, while the source broadcasts its message, the relays listen to the source (listening phase) and try to decode the source message. In the case that a relay decodes successfully before the destination, it enters the second phase (collaboration phase), in which it retransmits the message (details of the collaboration phase follow below). The source and all collaborating relays continue transmitting and the destination continues receiving until it has successfully decoded the data and sends an acknowledgment. Relay nodes may receive their information only from the source node (synchronous transmission protocol [15, Section III]) or from the source node and other relay nodes that have decoded earlier (asynchronous transmission protocol [15, Section IV]). Hence, in the asynchronous transmission protocol, relay nodes help each other to shorten individual listening phases. Furthermore, following the arguments in [15, Sections II and III.A], we assume direct-sequence code-division multiple access (CDMA) transmission where each relay node has a different spreading code available for transmission, which also enables the destination to identify the respective senders. Applying the idealization of orthogonal spreading codes arriving at the receiver, parallel source/relay-to-destination channels result and mutual information through different channels can be accumulated. If perfect orthogonality is violated, a performance penalty due to interference would result.

We apply rateless codes to protect messages against channel errors and an error detection mechanism (e.g. cyclic-redundancy check code) to terminate decoding [12], [15]. As in [8], [12], [15], we assume that CSI is only available at the receiver sides of a communication link. In such a practically relevant scenario the use of rateless codes is intended to achieve a relay-centric adaptation of the duration of the two communication phases to the instantaneous channel quality. Furthermore, source and relay nodes are assumed to transmit with the same power during the respective transmission phases [8], [12], [15].

B. Signal Combining Methods

Signal combining is performed during the collaboration phase at the destination node, and in the asynchronous transmission protocol also at relays which have not yet successfully decoded the source message. To enable more efficient signal combining methods, we extend the scheme from [15] in that we allow relays to transmit not only with their own spreading sequence but also with the spreading sequence allocated to the source. This spreading sequence re-use is a reasonable extension as (i) both resources are occupied during the collaboration phase anyhow, i.e., this extension does not drain any additional network resources, and (ii) the self-adaptivity

of the transmission scheme is maintained; that is, the re-use of the source spreading sequence at a relay does not require any coordination among nodes.

Next, to describe the combining methods, let us consider the basic example of a network with a single relay. We define the length-k source message vector $\boldsymbol{m}$ and the spreading sequences $\boldsymbol{s}_{\mathrm{S}}$ and $\boldsymbol{s}_{\mathrm{R}}$ applied at the source and relay[1], respectively. In the listening phase, the source transmits the length-n_{R} code vector $\boldsymbol{c}_{\mathrm{L}} = \boldsymbol{m}\boldsymbol{G}_{\mathrm{L}}$ applying spreading with $\boldsymbol{s}_{\mathrm{S}}$, where $\boldsymbol{G}_{\mathrm{L}}$ is the $k \times n_{\mathrm{R}}$ part of the generator matrix of the rateless code. Note that n_{R} is not decided prior to the transmission but is determined after the relay has successfully decoded the message $\boldsymbol{m}$.

We now proceed with the collaboration phase, i.e., we assume that the relay successfully decoded the source message before the destination. Let us define the length $(n - n_{\mathrm{R}})$ code vectors

$$\boldsymbol{c}_{\mathrm{C}} = \boldsymbol{m}\boldsymbol{G}_{\mathrm{C}} , \tag{1}$$

$$\boldsymbol{c}_{\mathrm{C}}^{1} = \boldsymbol{m}\boldsymbol{G}_{\mathrm{C}}^{1} , \tag{2}$$

where $n > n_{\mathrm{R}}$ is the number of coded bits received by the destination until successful decoding, and $\boldsymbol{G}_{\mathrm{C}}$ and $\boldsymbol{G}_{\mathrm{C}}^{1}$ are $k \times (n - n_{\mathrm{R}})$ generator matrices of the rateless codes used during the collaboration phase. The source node always applies $\boldsymbol{G}_{\mathrm{C}}$ to generate the vector $\boldsymbol{c}_{\mathrm{C}}$, which is transmitted using spreading with $\boldsymbol{s}_{\mathrm{S}}$. At the relay, the availability of two spreading sequences makes different signal combining schemes possible.

1) *Energy combining (EC)*: The relay node transmits the same signal as the source node, i.e., the relay applies $\boldsymbol{G}_{\mathrm{C}}$ and transmits message $\boldsymbol{c}_{\mathrm{C}}$ using $\boldsymbol{s}_{\mathrm{S}}$. Due to the different propagation delays of SD and RD channel, the destination can apply a Rake receiver to maximal-ratio (i.e., energy) combine the source and relay signals (cf. [15, Section III.A]). Then, decoding of the rateless code is done based on the total generator matrix $[\boldsymbol{G}_{\mathrm{L}}\ \boldsymbol{G}_{\mathrm{C}}]$.

2) *Information combining (IC)*: The relay re-encodes the source message using $\boldsymbol{G}_{\mathrm{C}}^{1}$ to obtain $\boldsymbol{c}_{C}^{1}$, which is transmitted using spreading code $\boldsymbol{s}_{\mathrm{R}}$. Due to the different spreading codes, the destination can distinguish between source and relay signals (cf. [15, Section III.A]). The rateless code uses generator matrix $[\boldsymbol{G}_{\mathrm{L}}\ \boldsymbol{G}_{\mathrm{C}}\ \boldsymbol{G}_{\mathrm{C}}^{1}]$ for decoding; that is, SD and RD are information combined.

3) *Mixed combining (MC)*: The relay node generates $\boldsymbol{c}_{\mathrm{C}}$ and $\boldsymbol{c}_{\mathrm{C}}^{1}$ and simultaneously transmits these messages using spreading with $\boldsymbol{s}_{\mathrm{S}}$ and $\boldsymbol{s}_{\mathrm{R}}$, respectively. To keep the total transmit power constant, the signal using $\boldsymbol{s}_{\mathrm{S}}$ is assigned a fraction $r \in [0, 1]$ and the signal using $\boldsymbol{s}_{\mathrm{R}}$ is transmitted with a fraction $1-r$ of the relay

[1]If we consider a single-relay network, we drop the relay index and write R and not R_1 for convenience.

transmit power, respectively. At the destination node, the source and relay signals that are transmitted with $\boldsymbol{s}_{\mathrm{S}}$ are energy combined, while the relay signal transmitted with $\boldsymbol{s}_{\mathrm{R}}$ is used for information combining. Hence, decoding is performed based on $[\boldsymbol{G}_{\mathrm{L}}\ \boldsymbol{G}_{\mathrm{C}}\ \boldsymbol{G}_{\mathrm{C}}^{1}]$, with EC applied for the $\boldsymbol{G}_{\mathrm{C}}$ part.

Note that regardless of the combining scheme, the relay sends a parity vector of length $(n - n_{\mathrm{R}})$, i.e., $\boldsymbol{c}_{\mathrm{C}}$ or $\boldsymbol{c}_{\mathrm{C}}^{1}$, that is different from the vector of n_{R} parity symbols transmitted during the listening phase. Hence, the considered rateless coded relay schemes always perform information combining across the two phases, which is also referred to as code combining [20] and coded cooperation [4] in the context of relaying using fixed-rate codes.

The generalization to relay networks with multiple relays is straightforward and has been investigated for transmission with Gaussian signaling and EC and IC in [15]. In IC, assuming N_{P} participating relays in the collaboration phase, relay i generates $\boldsymbol{c}_{\mathrm{C}}^{i} = \boldsymbol{m}\boldsymbol{G}_{\mathrm{C}}^{i}$, where $\boldsymbol{G}_{\mathrm{C}}^{i}$ has dimension $k \times (n - n_{\mathrm{R}_i})$ and n_{R_i} is the duration of the listening phase for relay i, and transmits $\boldsymbol{c}_{\mathrm{C}}^{i}$ using its unique spreading sequence $\boldsymbol{s}_{\mathrm{R}_i}$, $i = 1, \ldots, N_{\mathrm{P}}$. In MC, which is our extension of the pure EC and IC schemes, relay i divides its transmit power between transmitting $\boldsymbol{c}_{\mathrm{C}}^{i}$ using $\boldsymbol{s}_{\mathrm{R}_i}$ and $\boldsymbol{c}_{\mathrm{C}}$ using $\boldsymbol{s}_{\mathrm{S}}$ according to $r_i/(1 - r_i)$.

III. Analysis of Combining Schemes

In this section, we compare the three combining schemes in terms of achievable rates. As in the previous section, for clarity of exposition, we explain concepts considering the single-relay case ($N_{\mathrm{R}} = 1$) first and then generalize to the multiple-relay case.

A. Maximum Achievable Rate

1) Single-Relay Case: Let us denote the capacities[2] of the SR and SD channel by C_{SR} and C_{SD} respectively, and the capacity of the joint SD and RD channel during the collaboration phase by C_{Comb}. We have that $C_{\mathrm{SR}} = C(\gamma_{\mathrm{SR}})$ and $C_{\mathrm{SD}} = C(\gamma_{\mathrm{SD}})$, where $C(\gamma)$ is the constellation-constrained capacity (in bit per channel use) for, e.g., quadrature-amplitude modulation (QAM) or phase-shift keying (PSK) constellation at SNR γ. The capacity C_{Comb} depends on the applied combining scheme. Following the arguments from [8], [12], arbitrarily low error rate is achievable with a code of rate $R = k/n = R_{\max} - \delta$ for any $\delta > 0$, where $R_{\max}$ is given by

$$R_{\max} = \frac{C_{\mathrm{Comb}} C_{\mathrm{SR}}}{C_{\mathrm{SR}} - C_{\mathrm{SD}} + C_{\mathrm{Comb}}}\,. \tag{3}$$

[2]In slight abuse of denotation, capacity is defined as average mutual information for a given signal constellation, which is also known as constellation-constrained capacity [21, Section 3.5].

Note that $C_{\mathrm{SR}} > C_{\mathrm{SD}}$, since we assumed $n > n_{\mathrm{R}}$ and thus a collaboration phase is reached. Expression (3) intuitively follows from assuming equality in the two constraints

$$k \leq n_{\mathrm{R}} C_{\mathrm{SD}} + (k/R - n_{\mathrm{R}}) C_{\mathrm{Comb}} \,, \tag{4}$$

$$k \leq n_{\mathrm{R}} C_{\mathrm{SR}} \,, \tag{5}$$

for $R = R_{\max}$.

2) Multiple-Relay Case: Without loss of generality, we assume that N_{P} relays have participated in the collaboration until the destination has decoded the message and that relay R_j has decoded before relay R_i for $j < i$. The corresponding listening phase of relay i includes n_{R_i} sampling intervals. Then, we have the $N_{\mathrm{P}}+1$ constraints

$$k \leq n_{\mathrm{R}_1} C_{\mathrm{SD}} + \sum_{i=1}^{N_{\mathrm{P}}-1} \left(n_{\mathrm{R}_{i+1}} - n_{\mathrm{R}_i}\right) C_{\mathrm{Comb},i} + \left(k/R - n_{\mathrm{R}_{N_{\mathrm{P}}}}\right) C_{\mathrm{Comb},N_{\mathrm{P}}}, \tag{6}$$

$$k \leq n_{\mathrm{R}_1} C_{\mathrm{SR}_i} + \sum_{j=1}^{i-1} \left(n_{\mathrm{R}_{j+1}} - n_{\mathrm{R}_j}\right) C_{\mathrm{Comb},\mathrm{R}_i,j}, \quad i = 1, \ldots, N_{\mathrm{P}} \,. \tag{7}$$

In (6), $C_{\mathrm{Comb},i}$, $i = 1, \ldots, N_{\mathrm{P}}$, denotes the constrained capacity of the channel that is established during the collaboration phase between the source and i relays at the transmitting side and the destination at the receiving end applying signal combining. Similarly, in (7), $C_{\mathrm{Comb},\mathrm{R}_i,j}$, $j = 1, \ldots, i-1$, $i = 1, \ldots, N_{\mathrm{P}}$, is the constrained capacity of the channel when the source and j previously activated relays are transmitting and relay i is receiving and combining those signals. Expressions for these capacities will be given in the next section. While $C_{\mathrm{Comb},\mathrm{R}_i,j} = C_{\mathrm{SR}_i}$ for the synchronous transmission protocol, $C_{\mathrm{Comb},\mathrm{R}_i,j} \geq C_{\mathrm{SR}_i}$ in the asynchronous transmission protocol, since relays help each other to decode the source message. Setting (7) to equality allows us to solve for n_{R_i}, $i = 1, \ldots, N_{\mathrm{P}}$, and $R_{\max}$ is the rate R obtained from equality in (6). The number of active relays N_{P} is given by the smaller of the constraints $N_{\mathrm{P}} \leq N_{\mathrm{R}}$ and $n_{\mathrm{R}_{N_{\mathrm{P}}}} < n \leq n_{\mathrm{R}_{N_{\mathrm{P}}+1}}$.

$R_{\max}$ is an important measure as, in principle, the application of rateless codes provides the possibility of self-adaptation of the actual code rate arbitrarily close to $R_{\max}$. For brevity, we refer to $R_{\max}$ from (6) and (7) (which is given explicitly in (3) for the single-relay case) as the achievable rate or constrained capacity in the following.

B. Comparison of Combining Schemes

1) Single-Relay Case: Since EC benefits from SNR combining and IC uses parallel channels, the capacities C_{Comb} for the combining schemes from Section II-B in the single-relay case are given by[3]

$$C_{\mathrm{Comb}}^{\mathrm{EC}} = C(\gamma_{\mathrm{SD}} + \gamma_{\mathrm{RD}}) \tag{8}$$

$$C_{\mathrm{Comb}}^{\mathrm{IC}} = C(\gamma_{\mathrm{SD}}) + C(\gamma_{\mathrm{RD}}) \tag{9}$$

$$C_{\mathrm{Comb}}^{\mathrm{MC}} = C(\gamma_{\mathrm{SD}} + r\gamma_{\mathrm{RD}}) + C((1-r)\gamma_{\mathrm{RD}}) \; . \tag{10}$$

Furthermore, since $R_{\max}$ in (3) is strictly monotonically increasing in C_{Comb}, we wish to maximize C_{Comb} for given γ_{SD} and γ_{RD}. While for general constellations, e.g., QAM and PSK, the constellation-constrained capacity $C(\gamma)$ cannot be expressed in closed form [21, Section 3.5], we know from the relation between mutual information and the minimum mean-square error (MMSE) when estimating the transmitted signal point from the received signal and the strict monotonicity of the MMSE with respect to the SNR γ [22, Theorem 1] that $C(\gamma)$ is a strictly concave function of γ [22, Appendix A]. The following lemma is useful to compare the capacities (8)-(10).

Lemma 3.1: Consider the constellation-constrained capacity $C(\gamma)$ and SNR values $a, b, c > 0$. Then,

$$C(a+b) + C(c) > C(c+b) + C(a) \quad \Leftrightarrow \quad c > a \; .$$

Proof: Denote the derivative of $C(\gamma)$ by $C'(\gamma)$. Since $C(\gamma)$ is strictly concave and increasing, the slope $C'(\gamma)$ is strictly decreasing. Hence,

$$\begin{aligned} C(a+b) + C(c) > C(c+b) + C(a) \quad &\Leftrightarrow \quad C(a+b) - C(a) > C(c+b) - C(c) \\ &\Leftrightarrow \quad \int_{a}^{a+b} C'(x)\mathrm{d}x > \int_{c}^{c+b} C'(x)\mathrm{d}x \\ &\Leftrightarrow \quad c > a \end{aligned}$$

■

Theorem 3.2: For general finite-size constellations, the capacities of the combining channels satisfy

$$C_{\mathrm{Comb}}^{\mathrm{EC}} < \begin{cases} C_{\mathrm{Comb}}^{\mathrm{IC}}, & \text{for all } (\gamma_{\mathrm{SD}} > 0, \gamma_{\mathrm{RD}} > 0) \\ C_{\mathrm{Comb}}^{\mathrm{MC}}, & \text{for all } (\gamma_{\mathrm{SD}} > 0, \gamma_{\mathrm{RD}} > 0, r < 1) \end{cases} , \tag{11}$$

$$C_{\mathrm{Comb}}^{\mathrm{IC}} < C_{\mathrm{Comb}}^{\mathrm{MC}} \text{ if and only if } (1-r)\gamma_{\mathrm{RD}} > \gamma_{\mathrm{SD}} \; . \tag{12}$$

[3]Note that we do not penalize the degree-of-freedom expansion necessary to achieve orthogonal SD and RD channels, since it is the underlying assumption, as in [15], that this expansion is done (e.g. using spreading sequences) no matter what combining is used.

Proof: Inequality (11) is the special case $a = 0$ in Lemma 3.1. Inequality (12) follows from Lemma 3.1 when substituting $a = \gamma_{\mathrm{SD}}$, $b = r\gamma_{\mathrm{RD}}$, and $c = (1-r)\gamma_{\mathrm{RD}}$. ■

From this theorem we conclude that MC can be superior to IC if and only if $\gamma_{\mathrm{RD}} > \gamma_{\mathrm{SD}}$. More specifically, any choice of $r \in (0, 1 - \gamma_{\mathrm{SD}}/\gamma_{\mathrm{RD}})$ will lead to $C^{\mathrm{MC}}_{\mathrm{Comb}} > C^{\mathrm{IC}}_{\mathrm{Comb}}$.

2) Multiple-Relay Case: The case of multiple relays is a straightforward extension of the single-relay case. For example, the MC capacity $C_{\mathrm{Comb},i}$ used in (6) is given by

$$C^{\mathrm{MC}}_{\mathrm{Comb},i} = C\left(\gamma_{\mathrm{SD}} + \sum_{j=1}^{i} r_j \gamma_{\mathrm{R}_j\mathrm{D}}\right) + \sum_{j=1}^{i} C\left((1-r_j)\gamma_{\mathrm{R}_j\mathrm{D}}\right) \ , \tag{13}$$

from which EC and IC follow as special cases for $r_j = 1$ and $r_j = 0$, $j = 1, \ldots, i$, respectively. Similarly, the MC capacity $C_{\mathrm{Comb},\mathrm{R}_i,j}$ in (7) for the transmission to relay R_i in the asynchronous protocol reads

$$C^{\mathrm{MC}}_{\mathrm{Comb},\mathrm{R}_i,j} = C\left(\gamma_{\mathrm{SR}_i} + \sum_{k=1}^{j} r_k \gamma_{\mathrm{R}_k\mathrm{R}_i}\right) + \sum_{k=1}^{j} C\left((1-r_k)\gamma_{\mathrm{R}_k\mathrm{R}_i}\right) \ . \tag{14}$$

Theorem 3.3: In the case of N_{P} active relays, MC and IC capacities satisfy

$$C^{\mathrm{IC}}_{\mathrm{Comb},N_{\mathrm{P}}} < C^{\mathrm{MC}}_{\mathrm{Comb},N_{\mathrm{P}}} \text{ if and only if } \exists i \in \{1, \ldots, N_{\mathrm{P}}\}\ (1-r_i)\gamma_{\mathrm{R}_i\mathrm{D}} > \gamma_{\mathrm{SD}} \ . \tag{15}$$

Proof: For the *if* part, let i^* such that $(1-r_{i^*})\gamma_{\mathrm{R}_{i^*}\mathrm{D}} > \gamma_{\mathrm{SD}}$, and let us choose $r_i = 0$ for $i = 1, \ldots, N_{\mathrm{P}}$ and $i \neq i^*$. Then, from Lemma 3.1 it follows that

$$\begin{aligned} C^{\mathrm{MC}}_{\mathrm{Comb},N_{\mathrm{P}}} &= C\left(\gamma_{\mathrm{SD}} + r_{i^*}\gamma_{\mathrm{R}_{i^*}\mathrm{D}}\right) + C\left((1-r_{i^*})\gamma_{\mathrm{R}_{i^*}\mathrm{D}}\right) + \sum_{\substack{i=1 \\ i\neq i^*}}^{N_{\mathrm{P}}} C(\gamma_{\mathrm{R}_i\mathrm{D}}) \\ &> C(\gamma_{\mathrm{SD}}) + C(\gamma_{\mathrm{R}_{i^*}\mathrm{D}}) + \sum_{\substack{i=1 \\ i\neq i^*}}^{N_{\mathrm{P}}} C(\gamma_{\mathrm{R}_i\mathrm{D}}) = C^{\mathrm{IC}}_{\mathrm{Comb},N_{\mathrm{P}}} \ . \end{aligned}$$

For the *only if* part, we assume $\forall i\ (1-r_i)\gamma_{\mathrm{R}_i\mathrm{D}} \leq \gamma_{\mathrm{SD}}$. Then, again using Lemma 3.1, we obtain

$$\begin{aligned} C^{\mathrm{MC}}_{\mathrm{Comb},N_{\mathrm{P}}} &= C\left(\gamma_{\mathrm{SD}} + r_1\gamma_{\mathrm{R}_1\mathrm{D}} + \sum_{i=2}^{N_{\mathrm{P}}} r_i\gamma_{\mathrm{R}_i\mathrm{D}}\right) + C\left((1-r_1)\gamma_{\mathrm{R}_1\mathrm{D}}\right) + \sum_{i=2}^{N_{\mathrm{P}}} C\left((1-r_i)\gamma_{\mathrm{R}_i\mathrm{D}}\right) \\ &\leq C(\gamma_{\mathrm{SD}}) + C\left(\gamma_{\mathrm{R}_1\mathrm{D}} + \sum_{i=2}^{N_{\mathrm{P}}} r_i\gamma_{\mathrm{R}_i\mathrm{D}}\right) + \sum_{i=2}^{N_{\mathrm{P}}} C\left((1-r_i)\gamma_{\mathrm{R}_i\mathrm{D}}\right) \ . \end{aligned}$$

Continuing this upper bounding based on Lemma 3.1, we arrive at the inequality $C^{\mathrm{MC}}_{\mathrm{Comb},N_{\mathrm{P}}} \leq C^{\mathrm{IC}}_{\mathrm{Comb},N_{\mathrm{P}}}$. ■

C. Optimization of Mixed Combining

We are now interested in the vector of power ratios $\boldsymbol{r} \doteq [r_1, \ldots, r_{N_{\mathrm{P}}}]$ that maximizes the capacity $C^{\mathrm{MC}}_{\mathrm{Comb},N_{\mathrm{P}}}$ when N_{P} relays are active. That is, we adjust $\boldsymbol{r}$ according to MC combining at the destination node. Optimiza-

tion of $\boldsymbol{r}$ also with respect to the inter-relay channels used in the asynchronous transmission protocol would require communication of CSI, which we refrain from in this work.

Considering (13) and the fact that $C(\gamma)$ is concave, we consider

$$\frac{\mathrm{d}C^{\mathrm{MC}}_{\mathrm{Comb},N_{\mathrm{P}}}}{\mathrm{d}r_i}\bigg|_{r_i=r_{\mathrm{opt},i}} = 0 \ , \quad i = 1,\ldots,N_{\mathrm{P}} \ , \tag{16}$$

to obtain the optimal vector $\boldsymbol{r}_{\mathrm{opt}} \doteq [r_{\mathrm{opt},1},\ldots,r_{\mathrm{opt},N_{\mathrm{P}}}]$, which leads to the set of linear equations

$$\gamma_{\mathrm{SD}} + \sum_{j=1}^{N_{\mathrm{P}}} r_{\mathrm{opt},j}\gamma_{\mathrm{R}_j\mathrm{D}} - (1-r_{\mathrm{opt},i})\gamma_{\mathrm{R}_i\mathrm{D}} = 0 \ , \quad i = 1,\ldots,N_{\mathrm{P}} \ . \tag{17}$$

While the solution of (17) satisfies $r_{\mathrm{opt},i} \leq 1$, the condition $r_{\mathrm{opt},i} \geq 0$ is not always true for all $i = 1,\ldots,N_{\mathrm{P}}$. We thus have the following necessary and sufficient conditions for $\boldsymbol{r}_{\mathrm{opt}}$ [23, Section 4.4]:

$$\frac{\mathrm{d}C^{\mathrm{MC}}_{\mathrm{Comb},N_{\mathrm{P}}}}{\mathrm{d}r_i}\bigg|_{r_i=r_{\mathrm{opt},i}} = 0 \ , \text{ for all } r_{\mathrm{opt},i} > 0 \ , \tag{18a}$$

$$\frac{\mathrm{d}C^{\mathrm{MC}}_{\mathrm{Comb},N_{\mathrm{P}}}}{\mathrm{d}r_i}\bigg|_{r_i=r_{\mathrm{opt},i}} \leq 0 \ , \text{ for all } r_{\mathrm{opt},i} = 0 \ . \tag{18b}$$

For a small number of active relays (18) can be solved by inspection using (17). In the single-relay case we obtain the closed-form solution

$$r_{\mathrm{opt}} = \max\{0, (1-\gamma_{\mathrm{SD}}/\gamma_{\mathrm{RD}})/2\} \ . \tag{19}$$

We observe from (19) that $r_{\mathrm{opt}} = 0$, i.e., MC becomes identical to IC, only if $\gamma_{\mathrm{RD}} < \gamma_{\mathrm{SD}}$. Otherwise, the effect of MC is to equalize the effective SNRs $\gamma_{\mathrm{SD}} + r\gamma_{\mathrm{RD}}$ and $(1-r)\gamma_{\mathrm{RD}}$ as both become $(\gamma_{\mathrm{SD}} + \gamma_{\mathrm{RD}})/2$ for $r = r_{\mathrm{opt}}$.

Since (18) can only be evaluated at the destination node, where the ratios $\gamma_{\mathrm{R}_i\mathrm{D}}/\gamma_{\mathrm{SD}}$ are known, a low-rate feedback channel from the destination which conveys a quantized version of $\boldsymbol{r}_{\mathrm{opt}}$ to the relays is required. This feedback is alike the acknowledgment signal sent in rateless coded systems by the destination to terminate the transmission after successful decoding [12], [15], [24]. In Section V we also show results for the single- and two-relay cases that suggest that the effect of quantization of $\boldsymbol{r}_{\mathrm{opt}}$ on performance is negligible.

IV. Raptor Codes for DDF

In this section, we investigate the asymptotic performance of the rateless codes on relay channels using density evolution (DE) [16]. In particular, we specialize the capacity-based results from the previous section to the class of Raptor codes constructed from a given ensemble of LDPC and LT codes. To this end, we first refine the DE analysis for Raptor codes presented in [17] for direct source-to-destination communication and then generalize it to case of relay transmission using DDF as described in Section II. Furthermore, the DE analysis also allows us to optimize the degree distribution of the LT part of Raptor codes.

A. Density Evolution for Raptor Codes

1) Preliminaries: DE is an algorithm to track message densities in message-passing decoding of codes, most notably belief propagation (BP) decoding, with the goal of determining the SNR threshold above which arbitrarily small bit-error rate (BER) can be achieved. It builds on the concentration theorem according to which the decoder performance for code realizations converges to the expected value for the code ensemble in the limit of infinitely long codes assuming cycle-free code graphs. To simplify the algorithm, one-dimensional approximations of DE have been proposed, among which mean-value evolution [25] and information-content evolution [26] are the most popular.

These DE approximations have been applied to the analysis and design of Raptor codes in [27] and [17]. More specifically, in [27] the evolution of the message mean assuming Gaussian densities for all [25] or, as a more refined approach, some messages [28] has been derived for the LT part of the code, and in [17] information content evolution is considered for describing joint decoding of LT and LDPC precode of a Raptor code, again applying the Gaussian approximation for the distribution of messages. In particular, the interaction between LT and precode decoding is described by the exchange of extrinsic mutual information to track convergence in iterative decoding.

In the following, since we also apply joint decoding, we start from the approach in [17] and extend it in that we do not require the "pessimistic assumption" [17] that the graph of the precode is reinitialized each time the LT code passes its extrinsic information to the precode. We therefore expect to obtain a better match between predictions from DE and decoding results achieved with BP.

2) The DE Algorithm: Let $\iota(x) = \sum_i \iota_i x^{i-1}$, $\omega(x) = \sum_i \omega_i x^{i-1}$, $\lambda(x) = \sum_i \lambda_i x^{i-1}$, and $\rho(x) = \sum_i \rho_i x^{i-1}$ denote the edge degree distribution for LT input symbols, LT output symbols, precode variable nodes, and precode check nodes, respectively, and $I(x) = \sum_i I_i x^i$ and $\Lambda(x) = \sum_i \Lambda_i x^i$ the LT input symbol and precode variable node degree distribution, respectively (cf. [17], [27]). The information content for messages from LT variable nodes, LT check nodes, precode variable nodes, and precode check nodes is denoted as L_{v}, L_{c}, P_{v}, and P_{c}, respectively. Furthermore, L_{e} and P_{e} represent the extrinsic information delivered by the LT code to the precode and vice versa, and C_{v} is the initial information content coming from the channel. The joint decoding graph for the Raptor code is illustrated in the top part of Figure 2, which also shows the information content variables. Finally, we use the superscript "$.^{(\ell)}$" to denote the decoding iteration count and define $J(x)$ as the constellation-constrained capacity of the binary-input AWGN channel with noise variance $2/x$.

Then we can formulate the following update equations for the information content for the LT code:

$$L_{\mathrm{v}}^{(\ell)} = \sum_i \iota_i J\left((i-1)\,J^{-1}(L_{\mathrm{c}}^{(\ell-1)}) + J^{-1}(P_{\mathrm{e}}^{(\ell-1)})\right) \tag{20}$$

$$L_{\mathrm{c}}^{(\ell)} = 1 - \sum_i \omega_i J\left((i-1)\,J^{-1}(1-L_{\mathrm{v}}^{(\ell)}) + J^{-1}(1-C_{\mathrm{v}})\right)\,. \tag{21}$$

The decoding of the precode is described by

$$P_{\mathrm{v}}^{(\ell)} = \sum_i \lambda_i J\left((i-1)J^{-1}(P_{\mathrm{c}}^{(\ell-1)}) + J^{-1}(L_{\mathrm{e}}^{(\ell-1)})\right) \tag{22}$$

$$P_{\mathrm{c}}^{(\ell)} = 1 - \sum_i \rho_i J\left((i-1)J^{-1}(1-P_{\mathrm{v}}^{(\ell)})\right)\,. \tag{23}$$

After each half-iteration the extrinsic information content is computed as

$$L_{\mathrm{e}}^{(\ell)} = \sum_i I_i J\left(iJ^{-1}(L_{\mathrm{c}}^{(\ell)})\right) \tag{24}$$

$$P_{\mathrm{e}}^{(\ell)} = \sum_i \Lambda_i J\left(iJ^{-1}(P_{\mathrm{c}}^{(\ell)})\right)\,. \tag{25}$$

We can eliminate the check node and extrinsic information content to obtain

$$L_{\mathrm{v}}^{(\ell)} = \phi_L(L_{\mathrm{v}}^{(\ell-1)}, P_{\mathrm{v}}^{(\ell-1)}) \tag{26}$$

$$P_{\mathrm{v}}^{(\ell)} = \phi_P(P_{\mathrm{v}}^{(\ell-1)}, L_{\mathrm{v}}^{(\ell-1)})\,, \tag{27}$$

which is our DE approximation. If for given degree distributions and channel input C_{v} the recursion reaches the fixed point $(L_{\mathrm{v}}, P_{\mathrm{v}}) = (1, 1)$, then we expect that decoding is successful. Denoting by $R_{\mathrm{pre}} = 1 - \frac{\int_0^1 \rho(x)\mathrm{d}x}{\int_0^1 \lambda(x)\mathrm{d}x}$ the precode rate and by α the average LT edge degree, for which $\iota(x) = \mathrm{e}^{\alpha(x-1)}$ [27], the corresponding *a posteriori* rate of the Raptor code (cf. [17, Eq. (1)]) is given by

$$R_{\mathrm{Rap}} = \frac{R_{\mathrm{pre}}}{\alpha \sum_i \frac{\omega_i}{i}}\,. \tag{28}$$

Conversely, if another fixed point is reached in (26), (27), decoding is expected to fail. We observe from (21) that the information content L_{c} converges to mutual information C_{v} of the channel for $L_{\mathrm{v}} \to 1$.

To illustrate our proposed DE, Figure 4 presents the evolution of the information content $L_{\mathrm{v}}^{(\ell)}$ and $L_{\mathrm{c}}^{(\ell)}$ for the Raptor code with $\omega(x)$ from [14, Table I, 2nd column] over the binary-input AWGN channel with capacity $C = 0.48$ bit/(channel use) as function of the iteration number ℓ. We observe that decoding converges to $L_{\mathrm{v}} = 1$ and $L_{\mathrm{c}} = C_{\mathrm{v}}$, respectively, for rates up to $R = 0.453$ bit/(channel use), which thus are deemed achievable. On the other hand, information content converges to $L_{\mathrm{v}} < 1$ and $L_{\mathrm{c}} < C_{\mathrm{v}}$ for rates $R \geq 0.454$ bit/(channel use). Hence, we expect high error rates in this rate region.

B. Density Evolution over Relay Channels

We now extend the DE approximation to the case of DDF in relay channels. To this end, we need to consider the Tanner graph representation and the mutual information $C_{\rm v}$ provided from channel observations, which are different for the different combining schemes. Figure 2 shows the decoding graphs for EC, IC, and MC (top to bottom) assuming $N_{\rm P} = 1$ active relay. For simplicity, we will focus on this single-relay case in the following, and generalization to $N_{\rm P} > 1$ is straightforward.

In the previous section, we tacitly assumed that the channel observation messages are symmetric Gaussian distributed. Since we have AWGN channels, in the listening phase this assumption is true for binary modulation and a good approximation for bit-interleaved coded modulation with multilevel signaling and Gray labeling [29] (cf. [30] for other labelings). In the collaboration phase, the channel observation messages at the destination can be modelled by a Gaussian mixture distribution

$$p_{C_{\rm v}}(x) = \sum_{j=1}^{N_{\rm M}} p_j \mathcal{N}_{\rm sym}(\mu_j) \ , \tag{29}$$

where $\mathcal{N}_{\rm sym}(\mu)$ denotes the symmetric Gaussian probability density with mean μ and variance $2|\mu|$ [26] and $N_{\rm M}$ and p_j are the number of mixture components and their weights, respectively. Denoting by $f \doteq n_{\rm R}/n$ the fraction of the transmission interval required for listening, the following can immediately be inferred from the graph representation in Figure 2 and the description of the combining schemes in Sections II-B and III-B:

$$\text{EC:} \qquad N_{\rm M} = 2,\ (p_1, p_2) = (f, 1-f)\,,\ (\mu_1, \mu_2) = \left(J^{-1}(C_{\rm SD}), J^{-1}(C_{\rm Comb}^{\rm EC})\right) \tag{30}$$

$$\text{IC:} \qquad N_{\rm M} = 2,\ (p_1, p_2) = \left(\frac{1}{2-f}, \frac{1-f}{2-f}\right),\ (\mu_1, \mu_2) = \left(J^{-1}(C_{\rm SD}), J^{-1}(C_{\rm RD})\right) \tag{31}$$

$$\begin{aligned}\text{MC:} \qquad & N_{\rm M} = 3,\ (p_1, p_2, p_3) = \left(\frac{f}{2-f}, \frac{1-f}{2-f}, \frac{1-f}{2-f}\right), \\ & (\mu_1, \mu_2, \mu_3) = \left(J^{-1}(C_{\rm SD}), J^{-1}(C(\gamma_{\rm SD} + r\gamma_{\rm RD})), J^{-1}(C((1-r)\gamma_{\rm RD}))\right)\ .\end{aligned} \tag{32}$$

Then, taking the mixture density (29) into account, we need to re-write update equation (21) as

$$L_{\rm c}^{(\ell)} = 1 - \sum_{j=1}^{N_{\rm M}} p_j \sum_i \omega_i J\left((i-1)\, J^{-1}(1 - L_{\rm v}^{(\ell)}) + J^{-1}(1 - J(\mu_j))\right)\ . \tag{33}$$

Hence, for a given f, DE approximation can be performed according to (26) and (27) using the check-node update (33). To determine f for a given target relay-channel rate $R = k/n$, we first obtain the rate $R_{\rm Rap,SR} = k/n_{\rm R}$ from (28) through the DE approximation for the SR channel. Then, $f = n_{\rm R}/n = R/R_{\rm Rap,SR}$ can be used.

C. Optimized Degree Distribution

The DE approximation can also be used to optimize the output symbol edge degree distribution $\omega(x)$ of Raptor codes for cooperative communications considered here. Again, we will concentrate on the single-relay case, and then remark on the extension to multiple active relays. Furthermore, we hasten to say that such an optimization requires knowledge of *instantaneous* SNRs for all channels (SD, SR, RR, RD), and thus the purpose of optimization is to obtain performance benchmarks for Raptor codes with fixed degree distribution.

To optimize $\omega(x)$ we need to consider check-node information content. Substituting (20), (25) into (33) and (22), (24) into (23) gives us the coupled update equations

$$L_{\mathrm{c}}^{(\ell)} = \varphi_L(L_{\mathrm{c}}^{(\ell-1)}, P_{\mathrm{c}}^{(\ell-1)}, \{\mu_i\}) \tag{34}$$

$$P_{\mathrm{c}}^{(\ell)} = \varphi_P(P_{\mathrm{c}}^{(\ell-1)}, L_{\mathrm{c}}^{(\ell-1)}) \; . \tag{35}$$

Furthermore, to obtain a condition on $\omega(x)$ for a contracting mapping with fixed point $(L_{\mathrm{c}}, P_{\mathrm{c}}) = (\sum_{j=1}^{N_{\mathrm{M}}} p_j J(\mu_j), 1) \doteq (\tilde{R}, 1)$ that lends itself for efficient numerical solution, we replace (35) by the conservative approximation $P_{\mathrm{c}}^{(\ell)} = \varphi_P(0, L_{\mathrm{c}}^{(\ell)})$. This leads to the one-dimensional recursion

$$L_{\mathrm{c}}^{(\ell)} = \varphi_L(L_{\mathrm{c}}^{(\ell-1)}, \varphi_P(0, L_{\mathrm{c}}^{(\ell-1)}), \{\mu_i\}) \doteq \tilde{\varphi}(L_{\mathrm{c}}^{(\ell-1)}) \; , \tag{36}$$

which has been considered in [17] for non-relay communication with Raptor codes. Convergence to $L_{\mathrm{c}} = \tilde{R}$ is ensured by

$$\tilde{\varphi}(L_{\mathrm{c}}) > L_{\mathrm{c}} \quad \forall L_{\mathrm{c}} \in [0, \tilde{R}) \; . \tag{37}$$

Furthermore, [17] (see also [27, Section V]) suggests the following additional conditions to facilitate successful start of BP decoding away from $L_{\mathrm{c}} = 0$:

$$\tilde{\varphi}(0) > \varepsilon \; , \quad \lim_{L_{\mathrm{c}} \to 0} \tilde{\varphi}'(L_{\mathrm{c}}) > 1 \; , \tag{38}$$

where ε is some small positive constant. Adapting the above conditions to our situation of relay transmission, we obtain the optimization problem (39) shown on the next page for the single-relay channel, where (39g)-(39i) are the conditions for successful decoding at the relay. $\tilde{\varphi}_{\mathrm{SR}}(z)$ is the SR-channel version of (36) and α_{SR} denotes the average edge degree for input symbols of the SR-channel part of the LT code. From the graphs in Figure 2 we observe that $\alpha_{\mathrm{SR}} = f \cdot \alpha$ for EC and $\alpha_{\mathrm{SR}} = \frac{f}{2-f} \cdot \alpha$ for IC and MC. δ_i, $i = 1, 2, 3$, in (39d) and (39g) are small step-size and offset parameters to sample the interval in which $\tilde{\varphi}(z) > z$ and $\tilde{\varphi}_{\mathrm{SR}}(z) > z$ should hold, respectively, [17], [27].

$$\max_{\alpha,f} \frac{1}{\alpha \sum_i \frac{\omega_{\mathrm{opt},i}}{i}} \tag{39a}$$

$$\omega_{\mathrm{opt}}(x) = \operatorname*{argmin}_{\omega(x)} \sum_i \frac{\omega_i}{i} \tag{39b}$$

$$\text{s.t.} \quad \sum_i \omega_i = 1 \tag{39c}$$

$$\tilde{\varphi}(z) > z \quad \forall z \in [0, \delta_1, \ldots, \tilde{R} - \delta_2) \tag{39d}$$

$$\omega_1 \tilde{R} > \varepsilon \tag{39e}$$

$$\omega_2 \alpha \sum_{j=1}^{N_{\mathrm{M}}} p_j \mathrm{e}^{-J^{-1}(1-J(\mu_j))/4} > 1 \tag{39f}$$

$$\tilde{\varphi}_{\mathrm{SR}}(z) > z \quad \forall z \in [0, \delta_1, \ldots, C_{\mathrm{SR}} - \delta_3) \tag{39g}$$

$$\omega_1 C_{\mathrm{SR}} > \varepsilon \tag{39h}$$

$$\omega_2 \alpha_{\mathrm{SR}} \mathrm{e}^{-J^{-1}(1-C_{\mathrm{SR}})/4} > 1 \tag{39i}$$

Due to the approximation (36), the inner optimization (39b)-(39i) for $\omega_{\mathrm{opt}}(x)$ is a linear program, which can be solved using standard numerical tools, e.g., the CVX package [31]. The outer optimization (39a) with respect to α and f is a two-dimensional search. To reduce this to a one-dimensional search problem, and thus arrive at an optimization problem similar in complexity to those for non-relay transmission considered in [17], [27], we propose to select

$$f = \frac{R_{\max}}{C_{\mathrm{SR}}}. \tag{40}$$

That is, the relative durations of listening and collaboration phase are adjusted according to the corresponding channel capacities, which is the solution for $f = n_{\mathrm{R}}/n$ from (6), (7).

The generalization of (39) to the multiple-relay case leads to an $(N_{\mathrm{P}} + 1)$-dimensional search with respect to α and the relative durations $f_i = n_{\mathrm{R}_i}/n$ of the listening phases of the N_{P} active relays. However, applying the solution from (6), (7) for f_i for all relays $i = 1, \ldots, N_{\mathrm{P}}$, reduces the optimization to a one-dimensional search, and hence optimization of the degree distribution of the Raptor code can be performed computationally efficient (cf. [17], [27]).

V. Results and Discussion

In this section, we present numerical results to illustrate the performance of Raptor coded DDF relaying, compare the three combining schemes used at the destination node, and discuss the optimization of the degree distribution.

A. Parameters

As in most related works, we assume binary phase-shift keying (BPSK) modulation at the source and the relays. The default Raptor code, i.e., without optimization of $\omega(x)$, consists of a rate-0.95 regular LDPC code and an LT code generated using the degree distribution from [14, Table I, 2nd column].

We focus on $N_{\mathrm{P}} = 1$ and $N_{\mathrm{P}} = 2$ active relays as relevant example cases. The SR_i and $\mathrm{R}_i\mathrm{D}$ channels associated with the i-th relay ($i \in \{1, 2\}$) and the SD channel are modeled as flat Rayleigh fading with instantaneous SNRs $\gamma_{\mathrm{SR}_i} = G_{\mathrm{SR}_i}\gamma_{\mathrm{SD}}$ and $\gamma_{\mathrm{R}_i\mathrm{D}} = G_{\mathrm{R}_i\mathrm{D}}\gamma_{\mathrm{SD}}$, where G_{SR_i} and $G_{\mathrm{R}_i\mathrm{D}}$ denote the SNR gains of the SR_i and $\mathrm{R}_i\mathrm{D}$ channel with respect to the SD channel. For this purpose, we adopt the log-distance path-loss model $\gamma_{\mathrm{AB}} = c \cdot (d_{\mathrm{AB}})^{-\kappa}$ with distance d_{AB} between nodes A and B and path-loss exponent κ, so that (see [32, Section II] for the single-relay case)

$$G_{\mathrm{SR}_i} = [1 + \zeta_{\mathrm{R}_i}^2 - 2\zeta_{\mathrm{R}_i}\cos(\theta_{\mathrm{R}_i})]^{\kappa/2} , \tag{41}$$

$$G_{\mathrm{R}_i\mathrm{D}} = G_{\mathrm{SR}_i}/\zeta_{\mathrm{R}_i}^{\kappa} , \tag{42}$$

where

$$\zeta_{\mathrm{R}_i} \doteq \frac{d_{\mathrm{R}_i\mathrm{D}}}{d_{\mathrm{SR}_i}} \tag{43}$$

and θ_{R_i} is the angle of the line connecting source, relay R_i, and destination (see Figure 3). In the case of the asynchronous transmission protocol, the relay-to-relay link has the instantaneous SNR $\gamma_{\mathrm{R}_1\mathrm{R}_2} = G_{\mathrm{R}_1\mathrm{R}_2}\gamma_{\mathrm{SD}}$, for which the SNR gain follows from the geometry shown in Figure 3 as

$$G_{\mathrm{R}_1\mathrm{R}_2} = \left[\Big((G_{\mathrm{SR}_1})^{-\frac{1}{\kappa}}\cos(\vartheta_{\mathrm{R}_1}) - (G_{\mathrm{SR}_2})^{-\frac{1}{\kappa}}\cos(\vartheta_{\mathrm{R}_2})\Big)^2 + \Big((G_{\mathrm{SR}_1})^{-\frac{1}{\kappa}}\sin(\vartheta_{\mathrm{R}_1}) - (G_{\mathrm{SR}_2})^{-\frac{1}{\kappa}}\sin(\vartheta_{\mathrm{R}_1})\Big)^2 \right]^{-\kappa/2} \tag{44}$$

and

$$\cos(\vartheta_{\mathrm{R}_i}) = (G_{\mathrm{SR}_i})^{-\frac{1}{\kappa}}(1 - \zeta_{\mathrm{R}_i}\cos(\theta_{\mathrm{R}_i})) , \quad \sin(\vartheta_{\mathrm{R}_i}) = (G_{\mathrm{R}_i\mathrm{D}})^{-\frac{1}{\kappa}}\sin(\theta_{\mathrm{R}_i}) . \tag{45}$$

The relative instantaneous SNRs are thus specified by θ_{R_i} and ζ_{R_i}, $i = 1, 2$. If not stated otherwise, the optimal power allocation ratio $\boldsymbol{r} = \boldsymbol{r}_{\mathrm{opt}}$ as defined in Section III-C is applied for MC.

B. Results

1) Single-relay Network: We start with the single-relay case and select $\kappa = 4$, $\theta_{\mathrm{R}} = \pi$, and $\zeta_{\mathrm{R}} = 4/3$, so that $G_{\mathrm{SR}} = 15$ dB and $G_{\mathrm{RD}} = 10$ dB as an exemplary scenario. We evaluate the achievable rate $R_{\max}$ from (3) for the different combining schemes introduced in Section II-B. Figure 5 shows the numerical results in terms of the respective cumulative density functions (CDFs) for $R_{\max}$ (lines) for the average SNR $\bar{\gamma}_{\mathrm{SD}} = \mathcal{E}\{\gamma_{\mathrm{SD}}\} = 0$ dB. While, as expected, IC is superior to EC, we observe further significant improvements due to the proposed MC. In particular, MC achieves notably lower outage rates, i.e., the probability that a certain rate is not supported by the relay channel, for rates between $R_{\max} = 0.5$ to $R_{\max} = 0.8$ bit/(channel use), corresponding to the range of outage rates between 10 % and 80 %. Also included in this figure are CDF values (makers) for rates predicted by the DE analysis from Section IV-B for the default Raptor code. For ease of comparison, the obtained rates are multiplied with a factor of 1.1. The almost perfect match of the shifted CDFs from the DE and the CDFs for the capacity-based achievable rate shows that Raptor codes are an effective coding method to turn the capacity-gains due to improved signal combining into actual rate gains.

Figure 6 shows the average achievable rate $\bar{R}_{\max} = \mathcal{E}\{R_{\max}\}$ (solid lines), where averaging with respect to channel fading is done by means of Monte Carlo integration, as a function of the average SD channel SNR $\bar{\gamma}_{\mathrm{SD}}$ for the three combining schemes. The consistent advantage of MC over IC and EC is confirmed, and the gains in terms of average SNR can be on the order of 3 dB compared to EC and 1 dB with respect to IC. Also included in this figure are the rates predicted from DE analysis (dashed lines) and simulated rates using Raptor codes (dash-doted lines). For the latter, the input-word length is chosen as $k = 9500$ bits. Again, DE results follow closely the capacity-based results. In fact, the rate ratio of 1.1 established in Figure 5 also applies to the curves in this figure. It can further be seen from Figure 6 that DE well predicts the rates achieved with finite-length Raptor codes. A proper comparison of simulated and achievable rates reveals that the Raptor codes require an "overhead factor" [14], [15] $(1+\epsilon) = \frac{R_{\max}}{R_{\mathrm{Rap}}}$ consistently of about 1.15, which is quite remarkable considering the length of the codes and quite close to the 11% overhead predicted by DE assuming asymptotically long codes. We note that this overhead is practically independent of the combining scheme, which corroborates the usefulness of the proposed MC for improved performance in DDF relaying and the ability of Raptor codes to make use of the available mutual information regardless of the type of combining channel through which it is provided.

The markers in Figure 6 represent $\bar{R}_{\max}$ when r_{opt} from (19) is quantized using a size-2 codebook designed based on 1000 sample values for $\gamma_{\mathrm{SD}}/\gamma_{\mathrm{RD}}$ such that the mean-square error with respect to r_{opt} is minimized.

As can be seen, the performance of MC is hardly affected by quantization, which demonstrates that MC can be implemented with little extra feedback from the destination in addition to the feedback signaling successful decoding.

Next, we compare the average achievable rate $\bar{R}_{\max}$ for the different combining schemes as function of the distance ratio ζ_{R} assuming path-loss exponents $\kappa = 2$ and $\kappa = 4$, respectively, in Figure 7. The average SNR $\bar{\gamma}_{\mathrm{SD}} = 0$ dB is adjusted for the SD channel. Since the relay moves closer to the source as ζ_{R} increases, the percentage of collaboration increases for larger ζ_{R}. It can be seen that MC consistently achieves the highest rate. The gain of MC over IC is a function of both ζ_{R} and κ, and significant for not-too-large ζ_{R}, where often $\gamma_{\mathrm{RD}} > \gamma_{\mathrm{SD}}$ (see (12)). It disappears for $\zeta_{\mathrm{R}} \to \infty$, because MC converges towards IC as $\gamma_{\mathrm{RD}} \to \gamma_{\mathrm{SD}}$. The gain for pure IC over EC is monotonically increasing with the length of the collaboration phase. Note that the total transmit energy is independent of the combining scheme, since the duration of the collaboration phase only depends on the SR channel quality.

Figure 8 presents a 3-dimensional scatter plot of (i) $R_{\max}$ from (3) and (ii) the rate predicted by DE multiplied by the factor 1.1, at $\bar{\gamma}_{\mathrm{SD}} = 0$. The three axes correspond to the different combining schemes. It can be seen from the 2-dimensional projection of the points onto the (MC, IC)-plane that MC always achieves a higher or the same rate as IC. Likewise, the projection onto the (IC, EC)-plane confirms the superiority of IC over EC. Hence, MC is the scheme of choice not only on average, but for every realization of the relay channel. The almost perfect overlap of capacity and scaled DE results demonstrates the suitability of Raptor codes to adapt to the instantaneous channel conditions in DDF relaying.

2) Two-relay Network: We now turn to the two-relay case, for which we assume parameter sets ($\zeta_{\mathrm{R}_1} = 3/4$, $\zeta_{\mathrm{R}_2} = 3$, $\theta_{\mathrm{R}_1} = 5\pi/6$, $\theta_{\mathrm{R}_2} = \pi/2$) and ($\zeta_{\mathrm{R}_1} = 4/3$, $\zeta_{\mathrm{R}_2} = 1/4$, $\theta_{\mathrm{R}_1} = 5\pi/6$, $\theta_{\mathrm{R}_2} = \pi/2$). The corresponding scenarios are illustrated in Figure 3 as Topology A and B, respectively.[4] We assume the asynchronous transmission protocol and path-loss exponent $\kappa = 4$.

Evaluating (6) and (7) for 3000 channel realizations, Figure 9 shows the average achievable rate $\bar{R}_{\max}$ versus the average SNR of the SD link $\bar{\gamma}_{\mathrm{SD}}$ for the three combining methods. Similar to the single-relay case in Figure 6, we observe a clear advantage of MC over EC and IC for both sample topologies. Topology A enables an on average larger rate than Topology B, which is due to relay R_2 being relatively close to the destination node in Topology B, for which the DF protocol is known to be inefficient. But both topologies benefit from

[4]Note that the convention that R_i decodes before R_j for $i < j$ has only been made in Section III for ease of exposition. For the scenario considered in Figure 9, relay R_2 decodes before R_1 if $\gamma_{\mathrm{SR}_2} > \gamma_{\mathrm{SR}_1}$.

the asynchronous transmission protocol, as both relays are located in between source and destination node.

Figure 10 presents the CDFs for the achievable rates at SNR $\bar{\gamma}_{\mathrm{SD}}$ =0 dB. As for the single-relay case in Figure 5, the results from DE are also shown, where the obtained rates are multiplied with the factor of 1.1 to make the overlap with the capacity-based rates explicit. The results confirm the consistent advantages of MC over EC and IC and that Raptor codes are able to realize these gains with an absolute performance close to the pertinent capacity limit. The latter fact is further emphasized in Figure 11, in which average achievable rates $\bar{R}_{\max}$ from Figure 9 for Topology B are plotted together with rates predicted from DE and simulated rates using $k = 9500$. We observe that the DE curves for Raptor codes follow the capacity curves, and that an additional rate overhead of about 5% occurs due to using finite-length codes as well as approximations made in the DE analysis. Similar to Figure 6, the markers in Figure 11 refer to $\bar{R}_{\max}$ when the optimal vector $\boldsymbol{r}_{\mathrm{opt}}$ is quantized using a size-2 codebook for each element of $\boldsymbol{r}_{\mathrm{opt}}$ obtained from mean-square error minimization of $\boldsymbol{r}_{\mathrm{opt}}$ for 1000 channel realizations. The excellent match with the results for unquantized feedback of $\boldsymbol{r}_{\mathrm{opt}}$ indicates the robustness of MC to the effect of imperfect power allocation between EC and IC for combining.

3) Optimized Degree Distributions: Finally, we consider DDF with Raptor codes employing an LT output symbol edge degree distribution $\omega_{\mathrm{opt}}(x)$ optimized according to (39) for given instantaneous node-to-node channel SNRs. The rationale for this per-channel optimization is the provable non-existence of universally capacity-approaching Raptor codes for binary input AWGN channels [27], i.e., a Raptor code with a fixed degree distribution cannot be optimal for all channel realizations in the considered relay transmission. Figure 12 shows the scatter plot of the DE predicted rates for Raptor codes with $\omega_{\mathrm{opt}}(x)$ and Raptor codes with the degree distribution from [14, Table I, 2nd column]. The single-relay channel at $\bar{\gamma}_{\mathrm{SD}} = \{-5, 0, +5\}$ dB (again $G_{\mathrm{SR}} = 15$ dB, $G_{\mathrm{RD}} = 10$ dB) and MC at the destination are considered. As expected, the optimized Raptor code consistently improves the achievable rate. At the same time, the gains compared to using a fixed degree distribution are fairly small. This in turn is not overly surprising since possible gains are bounded by the capacity limit, which we have found to be on the order of only 10%. More specifically, notable gains are only seen for relatively high rates close to one, which is consistent with recent work on on-the-fly adaptation of the degree distribution of rateless codes in [33]. In summary, from the results we conclude that Raptor codes with a fixed degree distribution, in particular the degree distribution presented in [14], are already well suited to implement DDF and that their performance can only slightly further be improved by optimization.

VI. Conclusion

In this paper, we have elaborated on the use of rateless codes to implement dynamic decode-and-forward relaying for cooperative communications. We have proposed and optimized a new method for combining signals sent from source and relay nodes at the destination, which is a hybrid of energy and information combining and has been named mixed combining. To analyze achievable data rates using different signal combining methods and practical rateless codes, namely Raptor codes, we have derived the constrained-capacity limits and a density-evolution approximation, respectively. Our main findings are that mixed combining offers a notable increase in achievable data rate compared to energy and information combining and that Raptor codes with a fixed degree distribution enable us to approach these rates fairly closely, e.g. within about 15% for the experiments shown in this paper.

References

[1] A. Sendonaris, E. Erkip, and B. Aazhang, "User cooperation diversity — Part I and Part II," *IEEE Trans. Commun.*, vol. 51, no. 11, pp. 1927 – 1948, Nov. 2003.

[2] J. Laneman and G. Wornell, "Distributed space-time-coded protocols for exploiting cooperative diversity in wireless networks," *IEEE Trans. Inform. Theory*, vol. 49, no. 10, pp. 2415 – 2425, Oct. 2003.

[3] J. Laneman, D. Tse, and G. Wornell, "Cooperative diversity in wireless networks: Efficient protocls and outage behavior," *IEEE Trans. Inform. Theory*, vol. 50, no. 12, pp. 3062 – 3080, Dec. 2004.

[4] M. Janani, A. Hedayat, T. Hunter, and A. Nosratinia, "Coded cooperation in wireless communications: Space-time transmission and iterative decoding," *IEEE Trans. Signal Processing*, vol. 52, no. 2, pp. 362 – 371, Feb. 2004.

[5] G. Kramer, M. Gastpar, and P. Gupta, "Cooperative strategies and capacity theorems for relay networks," *IEEE Trans. Inform. Theory*, vol. 51, pp. 3037 – 3063, Sept. 2005.

[6] E. van der Meulen, "Three-terminal communication channels," *Adv. Appl. Probab.*, vol. 3, pp. 120 – 154, 1971.

[7] T. Cover and A. El Gamal, "Capacity theorems for the relay channel," *IEEE Trans. Inform. Theory*, vol. 25, pp. 572 – 584, Sept. 1979.

[8] P. Mitran, H. Ochiai, and V. Tarokh, "Space-time diversity enhancements using collaborative communications," *IEEE Trans. Inform. Theory*, vol. 51, no. 6, pp. 2041 – 2057, June 2005.

[9] M. Katz and S. Shamai (Shitz), "Transmitting to colocated users in wireless ad hoc and sensor networks," *IEEE Trans. Inform. Theory*, vol. 51, no. 10, pp. 3540 – 3563, Oct. 2005.

[10] K. Azarian, H. El Gamal, and P. Schniter, "On the achievable diversity-multiplexing tradeoff in half-duplex cooperative channels," *IEEE Trans. Inform. Theory*, vol. 51, no. 12, pp. 4152 – 4172, Dec. 2005.

[11] K. Raj Kumar and G. Caire, "Coding and decoding for the dynamic decode and forward relay protocol," *IEEE Trans. Inform. Theory*, vol. 55, no. 7, pp. 3186 – 3205, July 2009.

[12] J. Castura and Y. Mao, "Rateless coding for wireless relay channels," in *IEEE Intl. Symp. on Inform. Theory (ISIT)*, Adelaide, Australia, Sept. 2005, pp. 810 – 814.

[13] M. Luby, "LT codes," in *Proc. 43rd Annual IEEE Symp. on Foundations of Comp. Sc. (FOCS)*, Vancouver, BC, Canada, Nov. 2002, pp. 271–280.

[14] A. Shokrollahi, "Raptor codes," *IEEE Trans. Inform. Theory*, vol. 52, pp. 2551 – 2567, June 2006.

[15] A. Molisch, N. Mehta, J. Yedidia, and J. Zhang, "Performance of fountain codes in collaborative relay networks," *IEEE Trans. Wireless Commun.*, vol. 6, no. 11, pp. 4108 – 4119, Nov. 2007.

[16] T. Richardson and R. Urbanke, "The capacity of low-density parity-check codes under message-passing decoding," *IEEE Trans. Inform. Theory*, vol. 47, pp. 595 – 618, Feb. 2001.

[17] A. Venkiah, C. Poulliat, and D. Declercq, "Analysis and design of raptor codes for joint decoding using information content evolution," in *Proc. Int. Symp. Inform. Theory (ISIT)*, Nice, France, June 2007, pp. 421–425.

[18] A. Chakrabarti, A. Baynast, A. Sabharwal, and B. Aazhang, "Low density parity check codes for the relay channel," *IEEE J. Select. Areas Commun.*, vol. 25, no. 2, pp. 280–291, Feb. 2007.

[19] P. Razaghi and W. Yu, "Bilayer low-density parity-check codes for decode-and-forward in relay channels," *IEEE Trans. Inform. Theory*, vol. 53, no. 10, pp. 3723 – 3739, Oct. 2007.

[20] B. Zhao and M. Valenti, "Practical relay networks: A generalization of hybrid-ARQ," *IEEE J. Select. Areas Commun.*, vol. 23, pp. 7 – 18, Jan. 2005.

[21] E. Biglieri, *Coding for Wireless Channels*. New York: Springer Science+Business Media, Inc., 2005.

[22] A. Lozano, A. Tulino, and S. Verdú, "Optimum power allocation for parallel Gaussian channels with arbitrary input distributions," *IEEE Trans. Inform. Theory*, vol. 52, no. 7, pp. 3033 – 3051, July 2006.

[23] R. Gallager, *Information Theory and Reliable Communication*. New York: John Wiley & Sons, 1968.

[24] M. Luby, "LT codes," in *Proc. 43rd Annual IEEE Symp. on Foundations of Comp. Sc. (FOCS)*, Vancouver, BC, Canada, Nov. 2002, pp. 271–280.

[25] S.-Y. Chung, T. J. Richardson, and R. L. Urbanke, "Analysis of sum-product decoding of low-density parity-check codes using a Gaussian approximation," *IEEE Trans. Inform. Theory*, vol. 47, no. 2, pp. 657 – 670, Feb. 2001.

[26] A. Roumy, S. Guemghar, G. Caire, and S. Verdú, "Design methods for irregular repeat-accumulate codes," *IEEE Trans. Inform. Theory*, vol. 50, pp. 1711 – 1727, Aug. 2004.

[27] O. Etesami and A. Shokrollahi, "Raptor codes on binary memoryless symmetric channels," *IEEE Trans. Inform. Theory*, vol. 52, pp. 2033 – 2051, May 2006.

[28] M. Ardakani and F. R. Kschischang, "A more accurate one-dimensional analysis and design of irregular LDPC codes," *IEEE Trans. Commun.*, vol. 52, no. 12, pp. 2106 – 2114, Dec. 2004.

[29] A. Martinez, A. Guillén i Fàbregas, and G. Caire, "Error probability analysis of bit-interleaved coded modulation," *IEEE Trans. Inform. Theory*, vol. 52, no. 1, pp. 262–271, Jan. 2006.

[30] A. Kenarsari-Anhari and L. Lampe, "An analytical approach for performance evaluation of BICM transmission over Nakagami-m fading channels," *IEEE Trans. Commun.*, vol. 58, pp. 1090–1101, Apr. 2010.

[31] M. Grant and S. Boyd. (2009, June) CVX: Matlab software for disciplined convex programming (web page and software). [Online]. Available: http://stanford.edu/~boyd/cvx

[32] H. Ochiai, P. Mitran, and V. Tarokh, "Variable-rate two-phase collaborative communication protocols for wireless networks," *IEEE Trans. Inform. Theory*, vol. 52, no. 9, pp. 4299 – 4313, Sept. 2006.

[33] N. Bonello, R. Zhang, S. Chen, and L. Hanzo, "Reconfigurable rateless codes," *IEEE Trans. Wireless Commun.*, vol. 8, no. 11, pp. 5592 – 5600, Nov. 2009.

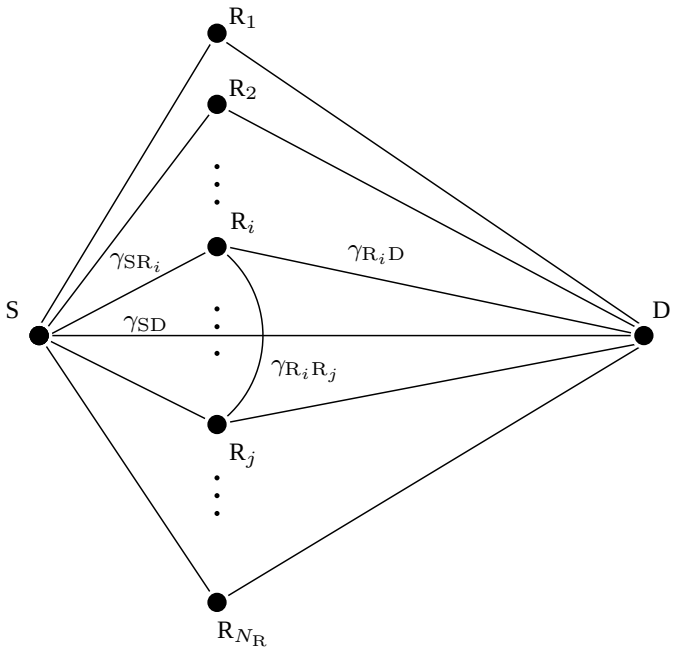

Fig. 1. Cooperative communications systems with source node S, destination node D, and N_{R} relays. The node-to-node channels are frequency flat fading AWGN channels with instantaneous signal-to-noise power ratios γ_{XY} between nodes X and Y.

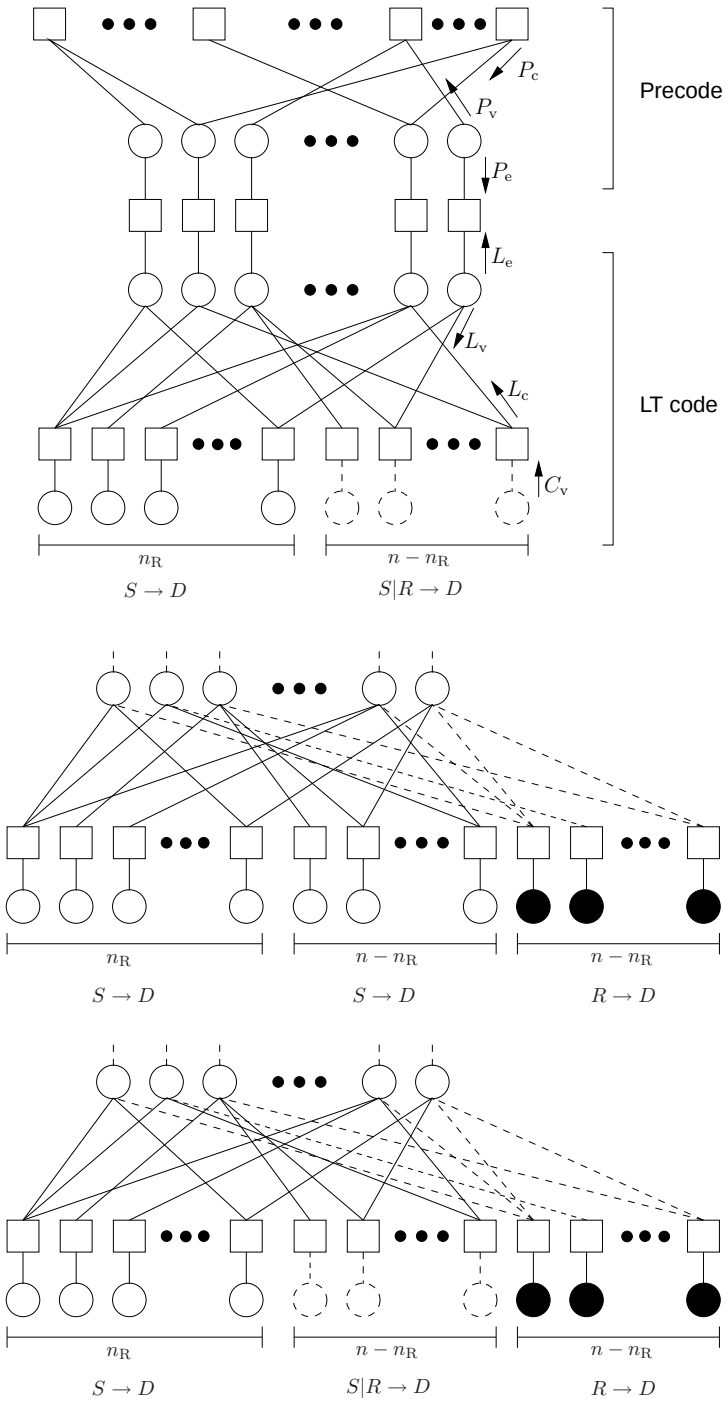

Fig. 2. Decoding graph for Raptor codes over single-relay channel for EC (top), IC (center), and MC (bottom) methods. Circles represent variable nodes and squares represent parity-check nodes. In case of LT output variables, solid white circles represent variables associated with samples received from the source in the listening phase, white dashed circles represent variables associated with the energy combined samples received from source and relay, black circles represent variables associated with samples received from the relay used for joint decoding (information combining). The top graph also includes the information content variables used for density evolution.

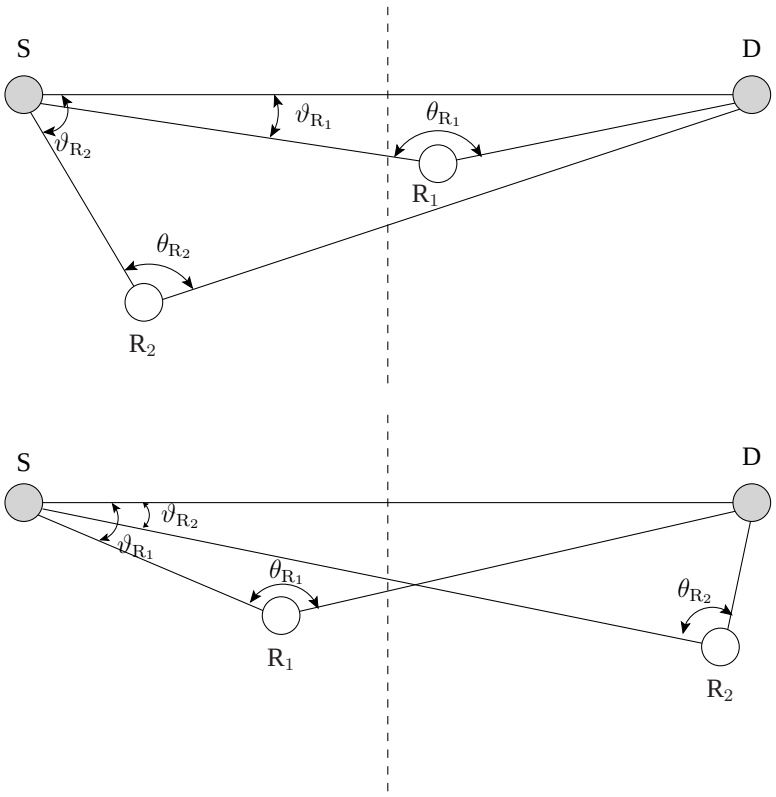

Fig. 3. Two exemplary topologies for four-node relay networks. Topology A (top) and topology B (bottom).

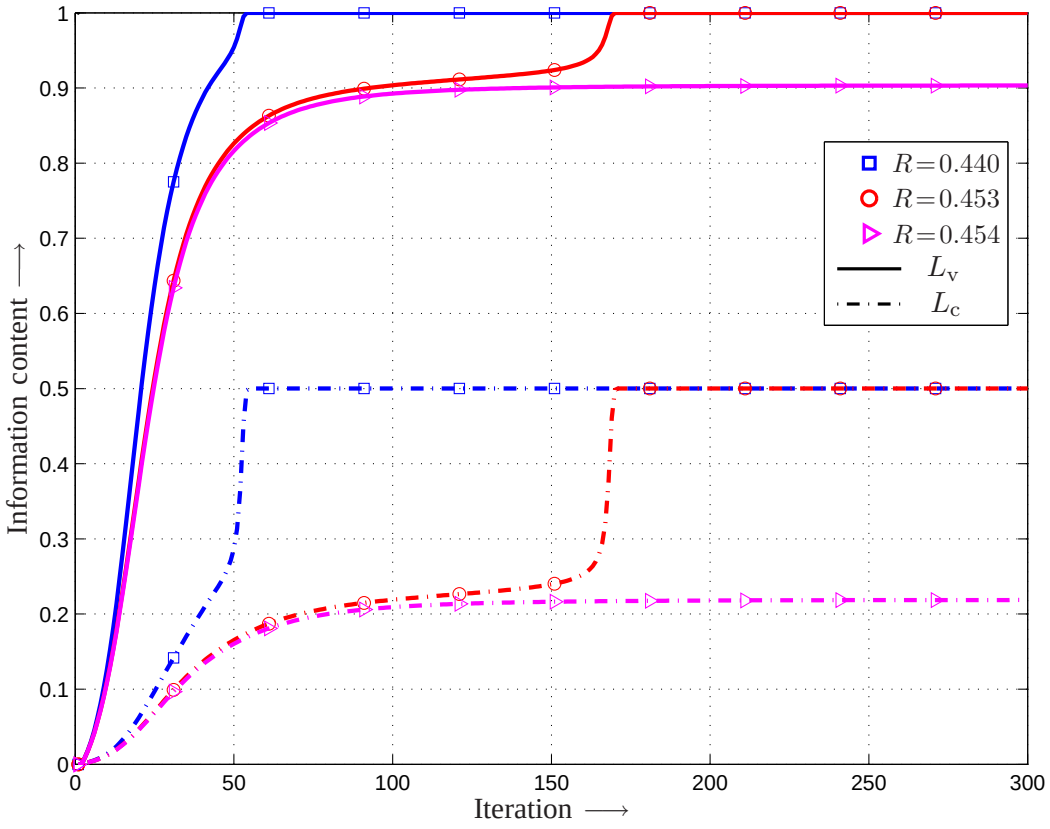

Fig. 4. Evolution of information content $L_{\mathrm{c}}^{(\ell)}$ and $L_{\mathrm{v}}^{(\ell)}$ of check and variable nodes, respectively, for Raptor codes with different *a posteriori* rates versus iteration number ℓ. AWGN channel with the capacity $C = 0.48$ bit/(channel use).

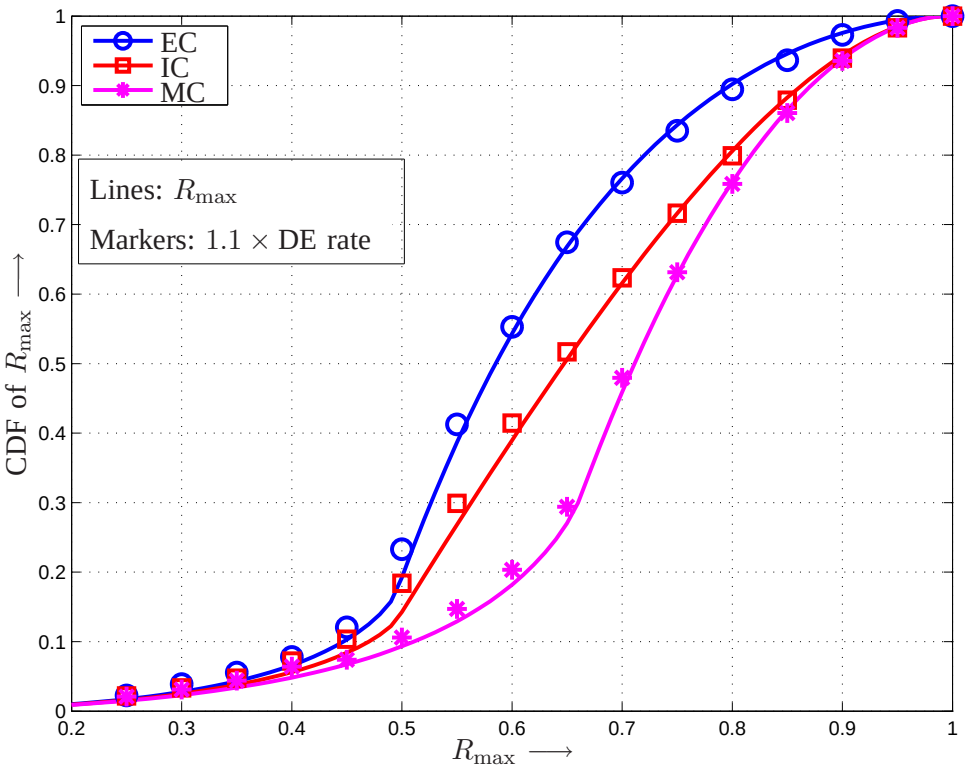

Fig. 5. CDF of achievable rate $R_{\max}$ from (3) (lines) and CDF for $1.1 \times$ (achievable rate with Raptor codes) determined with DE (markers). Single-relay case, $\bar{\gamma}_{\mathrm{SD}} = 0$ dB, $G_{\mathrm{SR}} = 15$ dB, $G_{\mathrm{RD}} = 10$ dB.

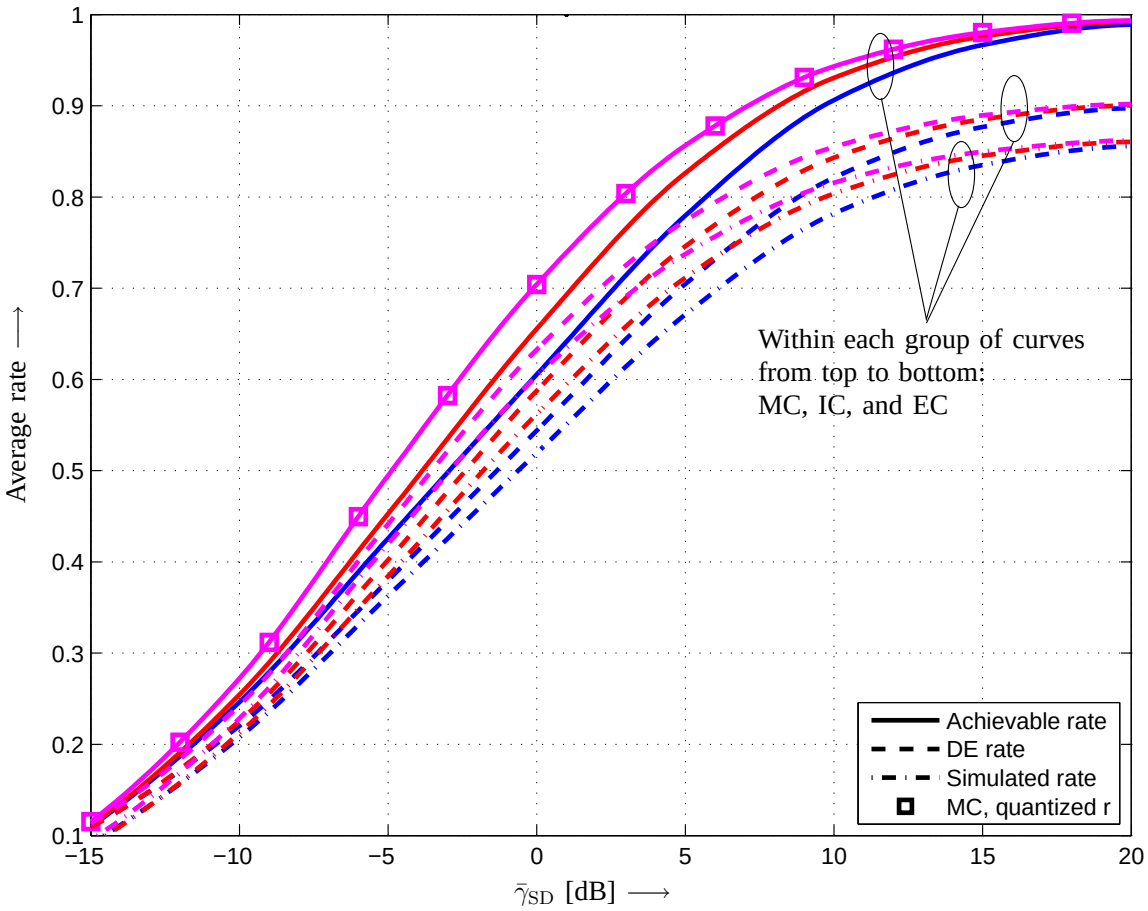

Fig. 6. Average achievable rate $\bar{R}_{\max}$ with $R_{\max}$ from (3), predicted rate for Raptor codes using DE, and simulated rate using a Raptor code with $k = 9500$ information symbols versus the average SD SNR $\bar{\gamma}_{\mathrm{SD}}$. Markers represent $\bar{R}_{\max}$ when r_{opt} from (19) is quantized. Single-relay case, $G_{\mathrm{SR}} = 15$ dB, $G_{\mathrm{RD}} = 10$ dB.

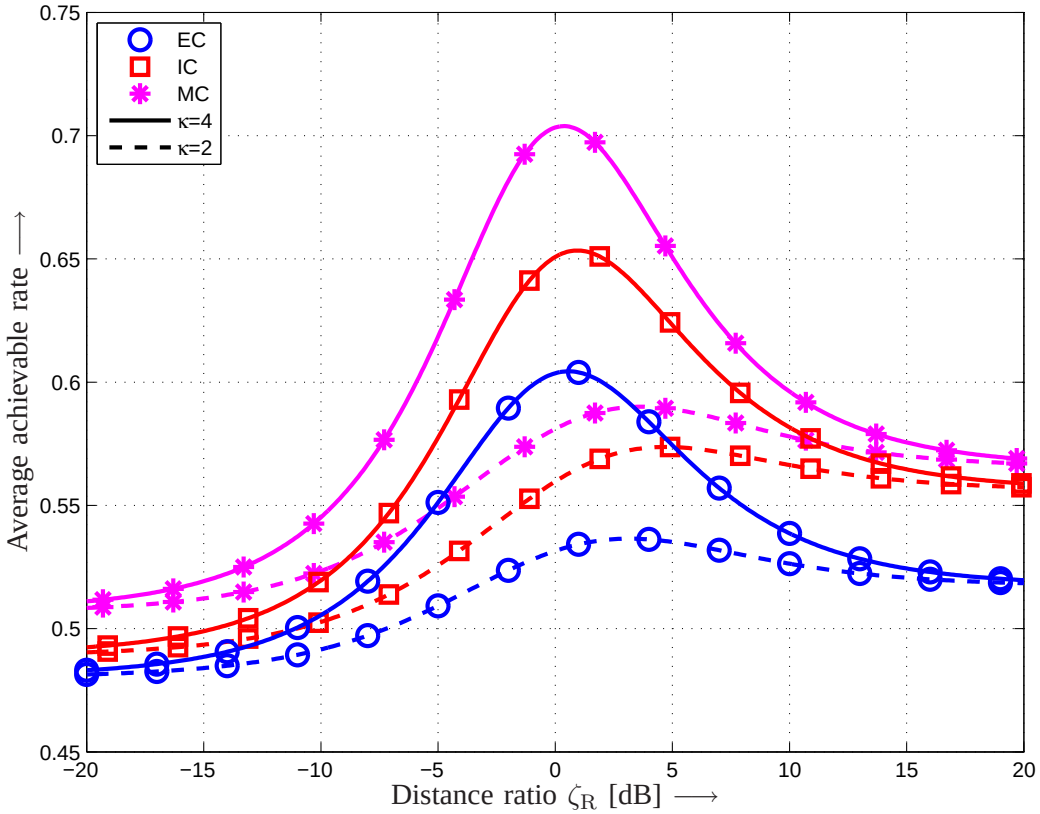

Fig. 7. Average achievable rate $\bar{R}_{\max}$ with $R_{\max}$ from (3) as function of the ratio ζ_{R} (43) and for path-loss exponent $\kappa = 4$ and $\kappa = 2$. Single-relay case, $\bar{\gamma}_{\mathrm{SD}} = 0$ dB.

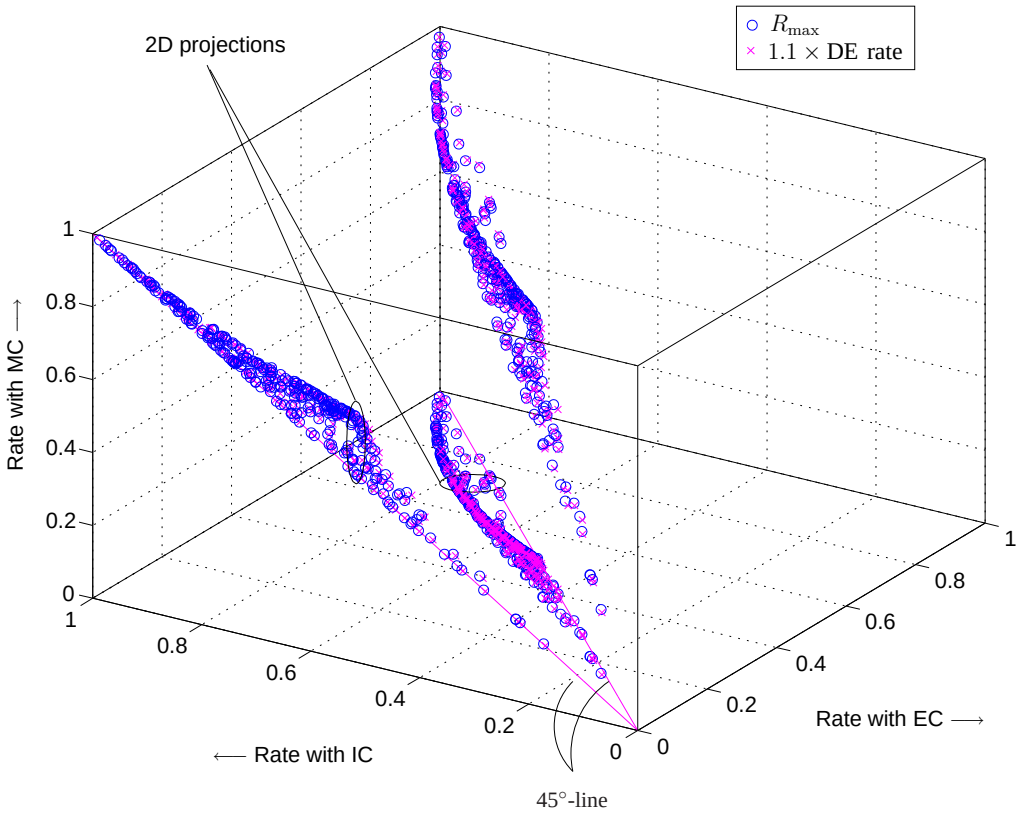

Fig. 8. Scatter plot of the $R_{\max}$ from (3) (circles) and $1.1 \times$ DE-predicted rates (crosses) with different combining methods for 300 channel realizations. Single-relay case, $\bar{\gamma}_{\mathrm{SD}} = 0$ dB, $G_{\mathrm{SR}} = 15$ dB, $G_{\mathrm{RD}} = 10$ dB.

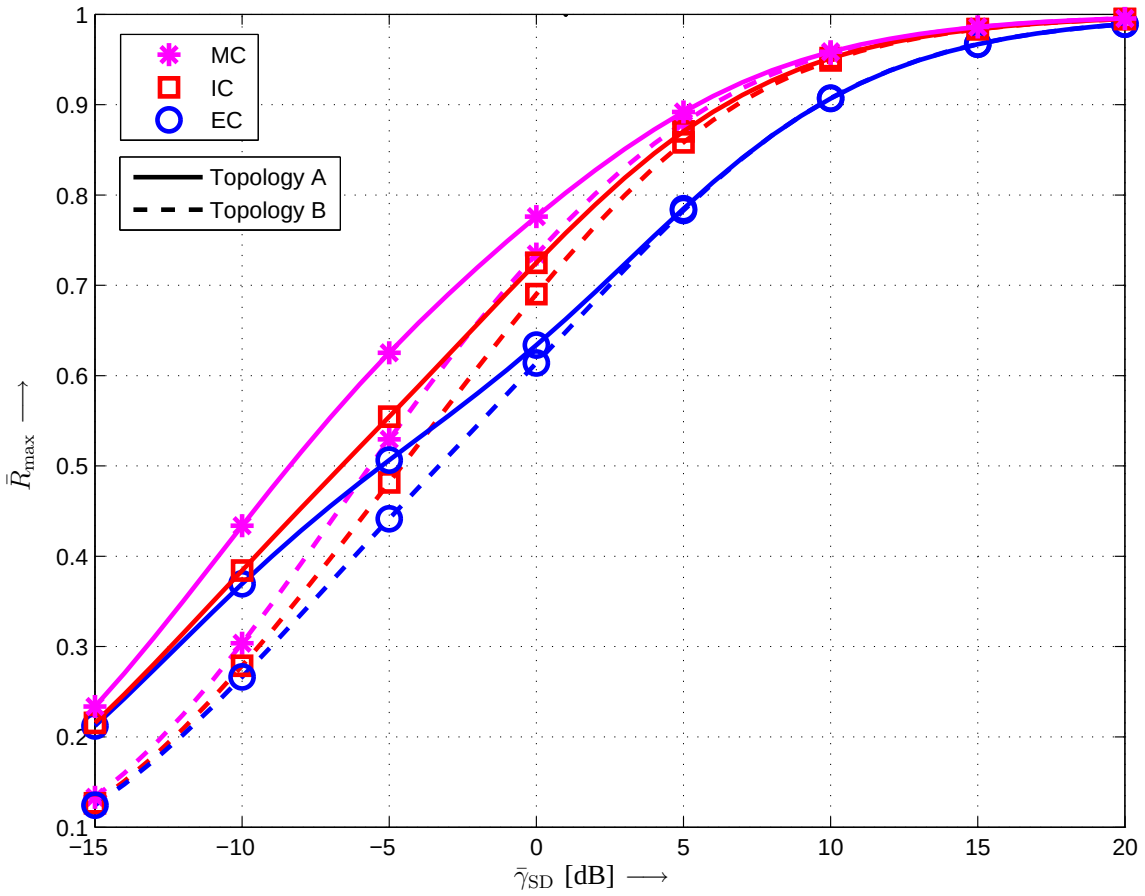

Fig. 9. Average achievable rate $\bar{R}_{\max}$ with $R_{\max}$ from (6) and (7) versus the average SD SNR $\bar{\gamma}_{\mathrm{SD}}$. Network with two-relays and Topologies A and B from Figure 3.

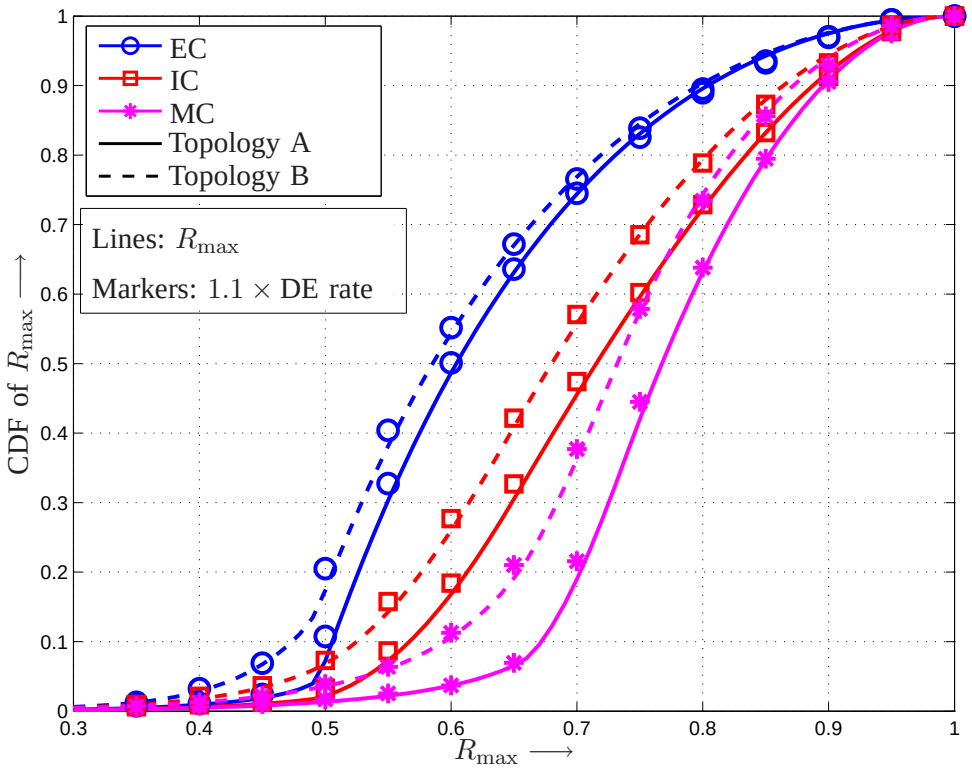

Fig. 10. CDF of achievable rate $R_{\max}$ from (6) and (7) (lines) and CDF for $1.1 \times$ (achievable rate with Raptor codes) determined with the DE (markers). Network with two-relays and Topologies A and B from Figure 3. $\bar{\gamma}_{\mathrm{SD}} = 0$ dB.

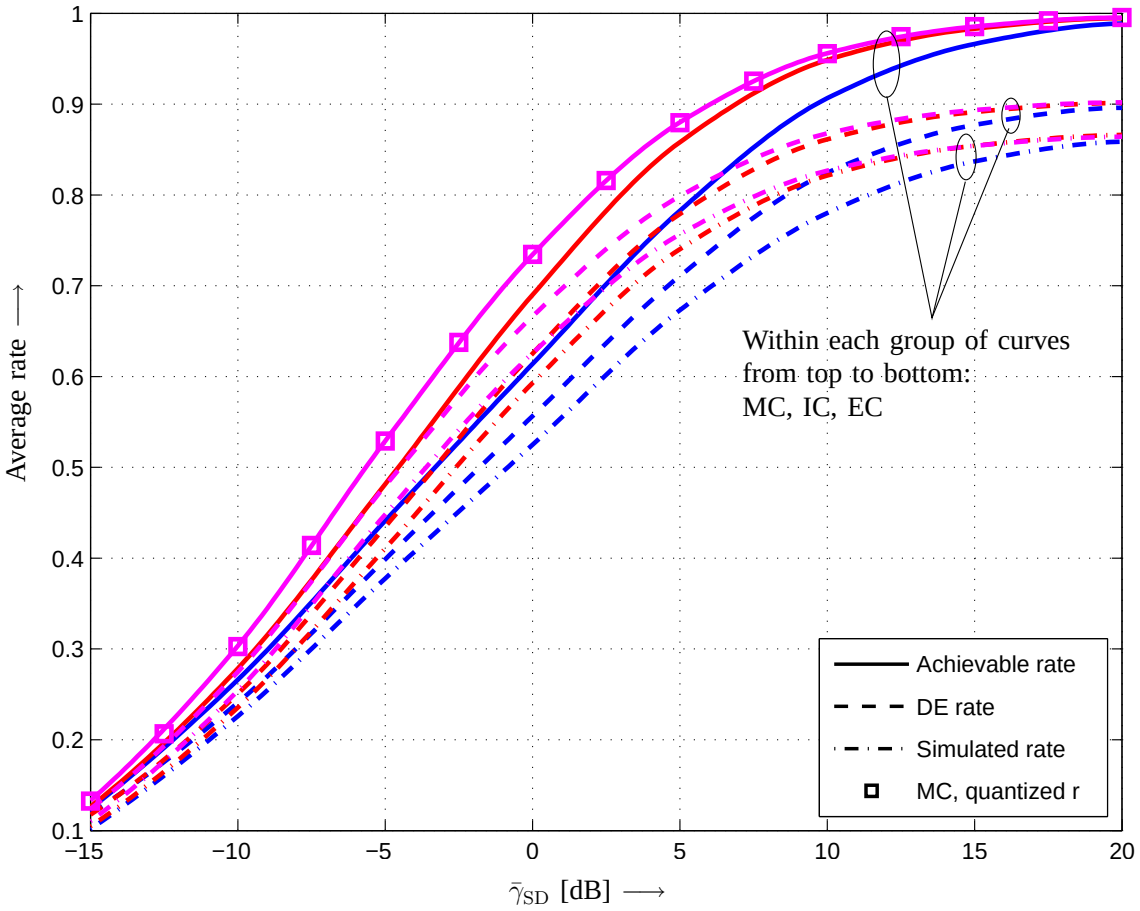

Fig. 11. Average achievable rate $\bar{R}_{\max}$ with $R_{\max}$ from (6) and (7), predicted rate for Raptor codes using DE, and simulated rate using a Raptor code with $k = 9500$ information symbols versus the average SD SNR $\bar{\gamma}_{\mathrm{SD}}$. Markers represent $\bar{R}_{\max}$ when r_{opt} from (19) is quantized. Network with two-relays and Topology B from Figure 3.

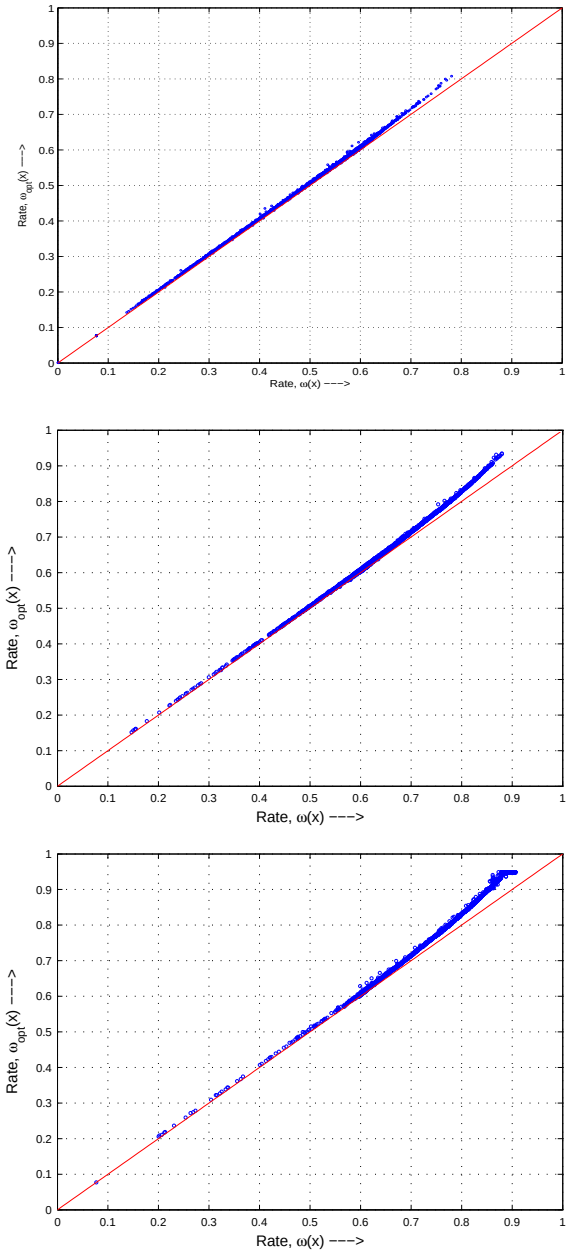

Fig. 12. Scatter plot of the DE predicted rate for Raptor codes with optimized degree distribution $\omega_{\rm opt}(x)$ and degree distribution $\omega(x)$ from [14, Table I, 2nd column]. Single-relay case, $\bar{\gamma}_{\rm SD} = -5$ dB (top), $\bar{\gamma}_{\rm SD} = 0$ dB (middle), and $\bar{\gamma}_{\rm SD} = 5$ dB (bottom), $G_{\rm SR} = 15$ dB, $G_{\rm RD} = 10$ dB, and mixed combining method.